High-Energy-Density Astrophysics in the Laboratory

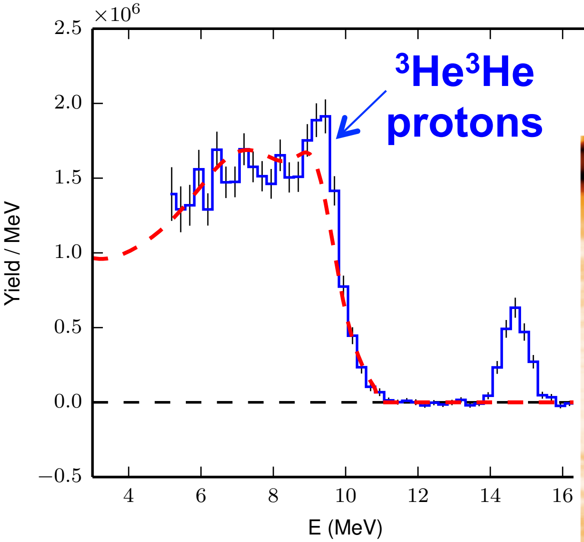

Plasma Nuclear Science

Hydrodynamic Instabilities

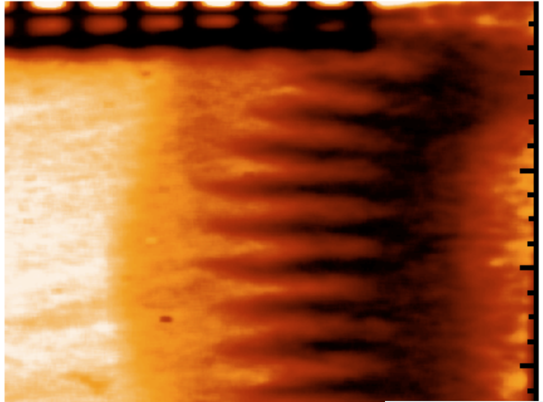

Pair Plasmas

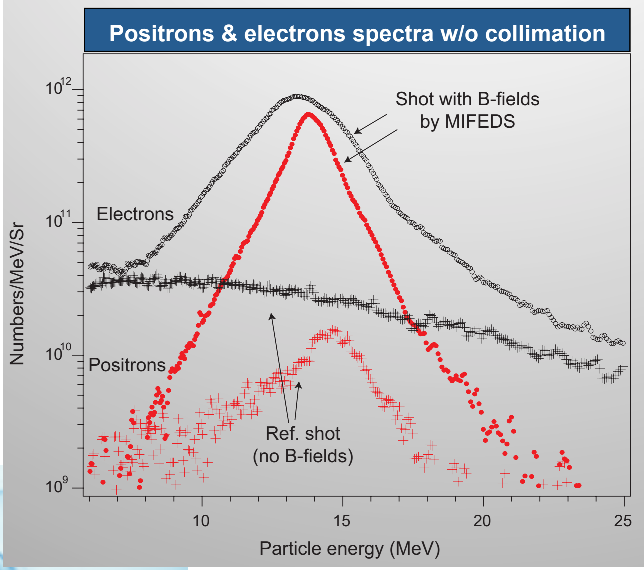

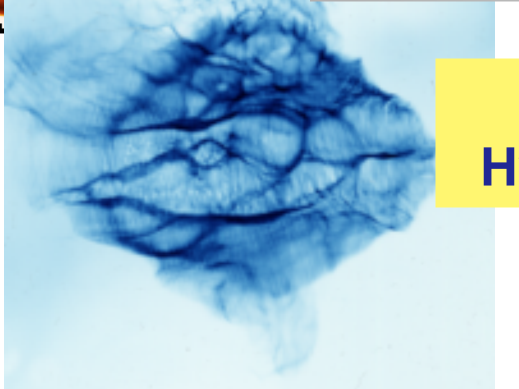

Magneto-Hydrodynamics

Mario Manuel
University of Michigan
National Undergraduate Fellowship Program
June 11th, 2015

Laboratory experiments provide a complimentary technique to investigate some astrophysical systems

- High-power laser facilities provide a unique opportunity to generate physical conditions similar to those in multiple astrophysical systems

- Laboratory results are directly scalable when similarity and geometric conditions hold between the two systems

- Experiments also allow for detailed benchmark comparisons with numerical calculations in relevant dynamic regimes

Outline

- High-Energy-Density (HED) Plasma
  - US facilities

Zylstra et al.
(MIT)

- Plasma Nuclear Science using ICF-like implosions
  - p-p chain at relevant Gamow energies

Drake,
Kuranz et al.
(UM)

- Laser-produced Magnetohydrodynamics
  - similarity conditions
  - Rayleigh-Taylor growth in core-collapse SNe

Park,
Huntington et al.
(LLNL)

- Laser-produced Jets
  - ‘collisionless’ shocks
  - supersonic jet dynamics

Manuel,
Kuranz et al.
(UM)

Chen et al.
(LLNL)

- Pair-Plasma Production
  - relativistic jets

- Summary

High-energy-density (HED) physics involves the study of systems having pressures > 1 Mbar

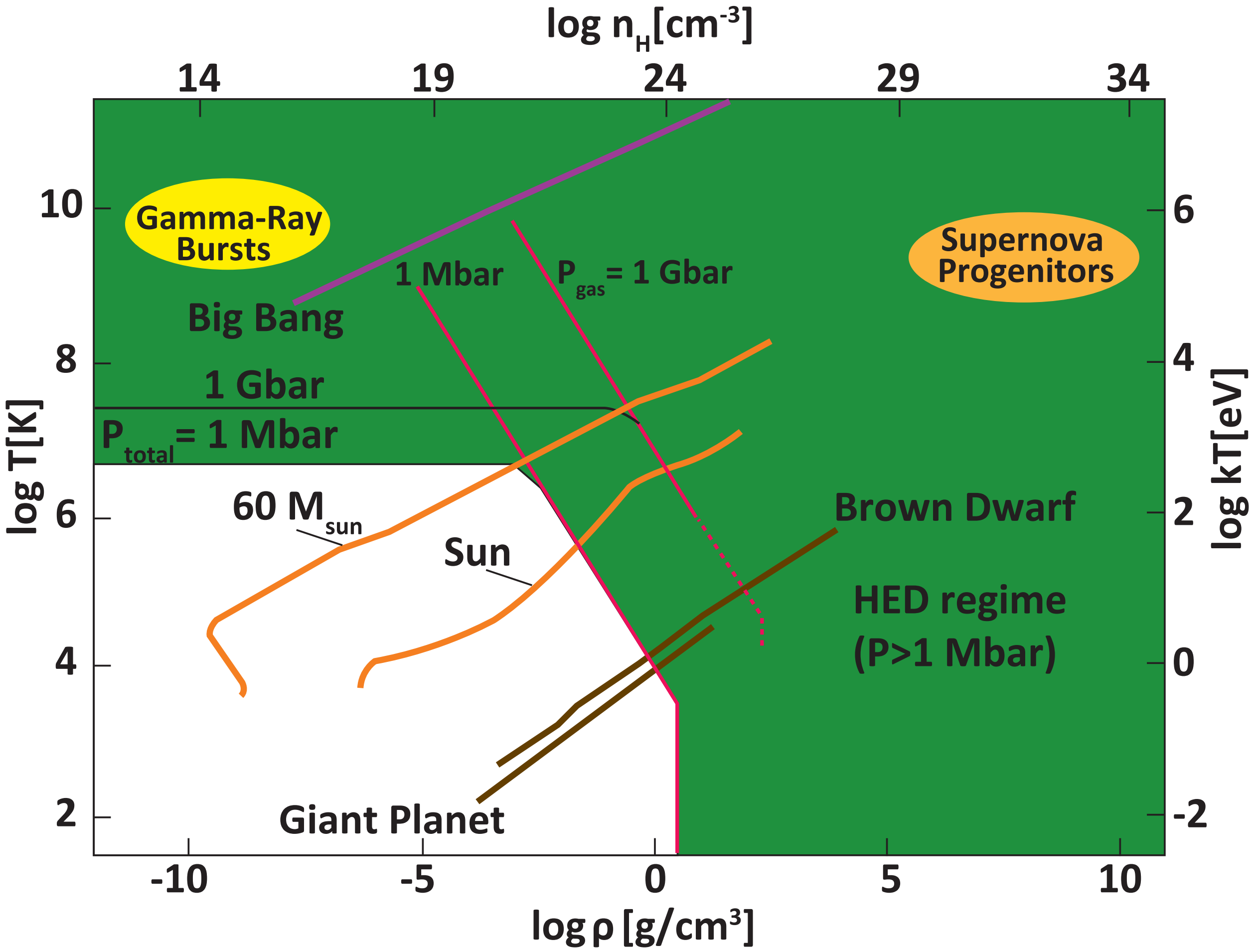

---

*Adapted from NRC committee on HEDP (2003)

Present-day laser facilities access a unique region in HED-relevant parameter space

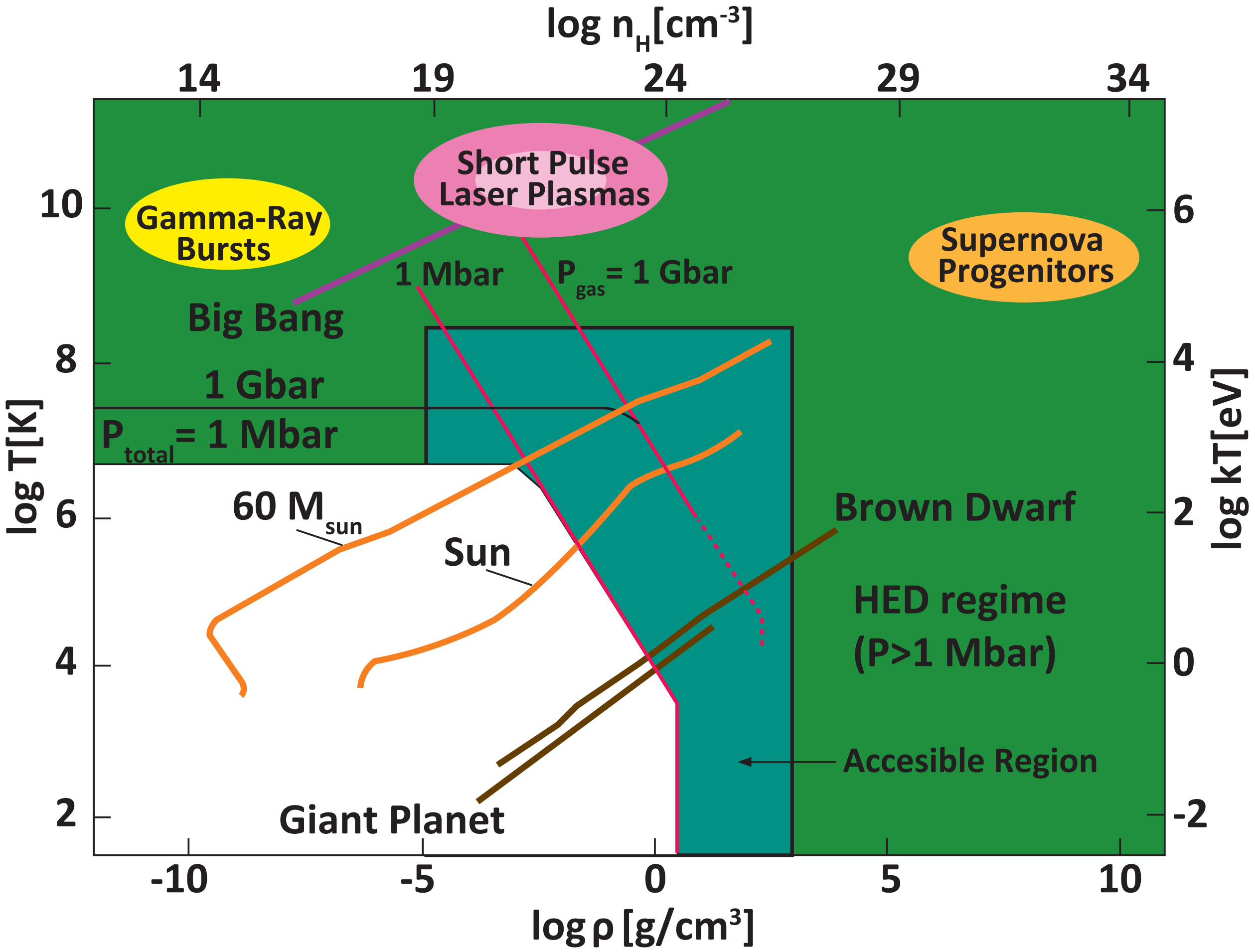

---

*Adapted from NRC committee on HEDP (2003)

Many experiments take place at the Omega Laser Facility

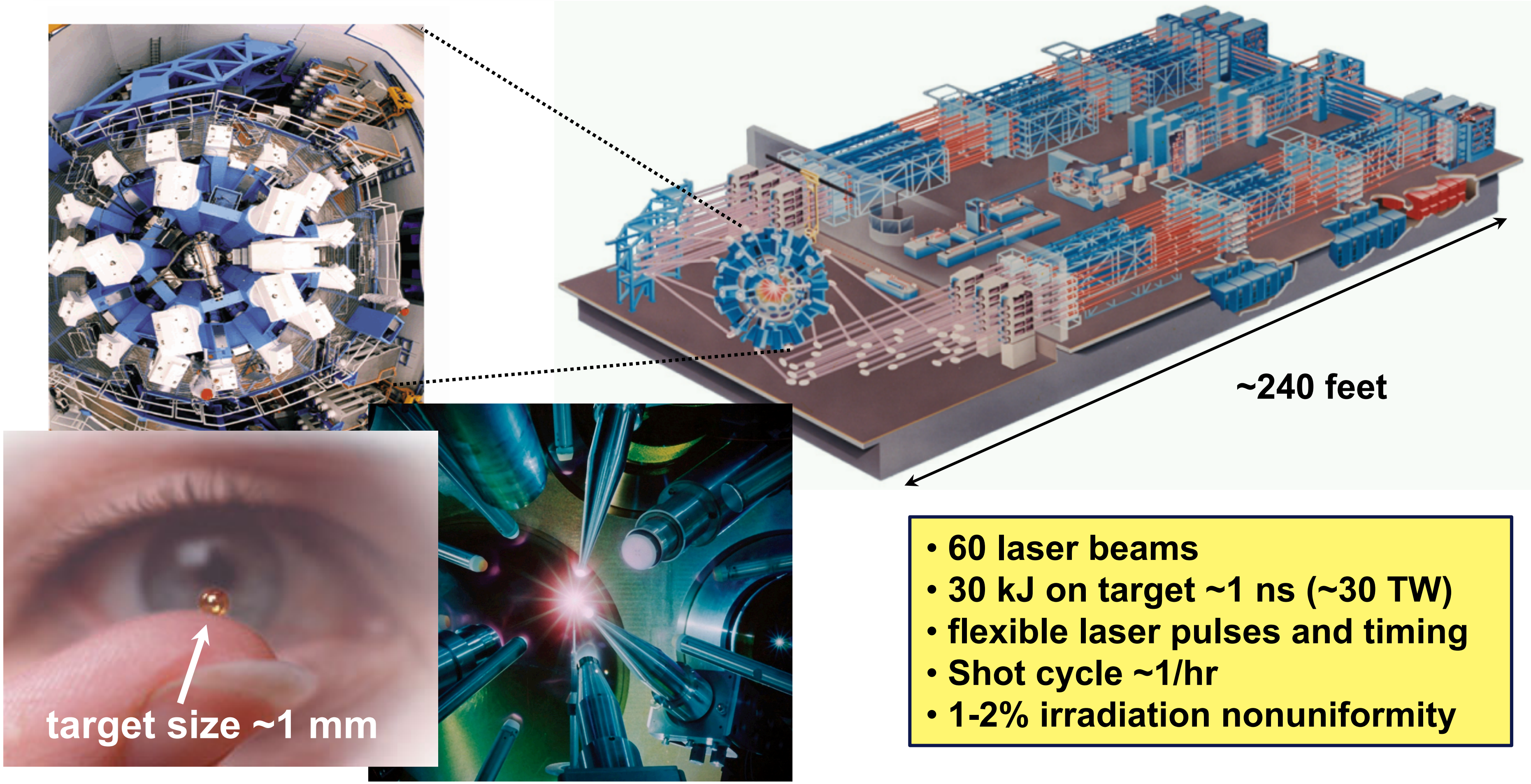

- **60 laser beams**
- **30 kJ on target ~1 ns (~30 TW)**
- **flexible laser pulses and timing**
- **Shot cycle ~1/hr**
- **1-2% irradiation nonuniformity**

---

*Boehly, Optics Comm. 133 (1997)

Next-gen experiments take place at the National Ignition Facility

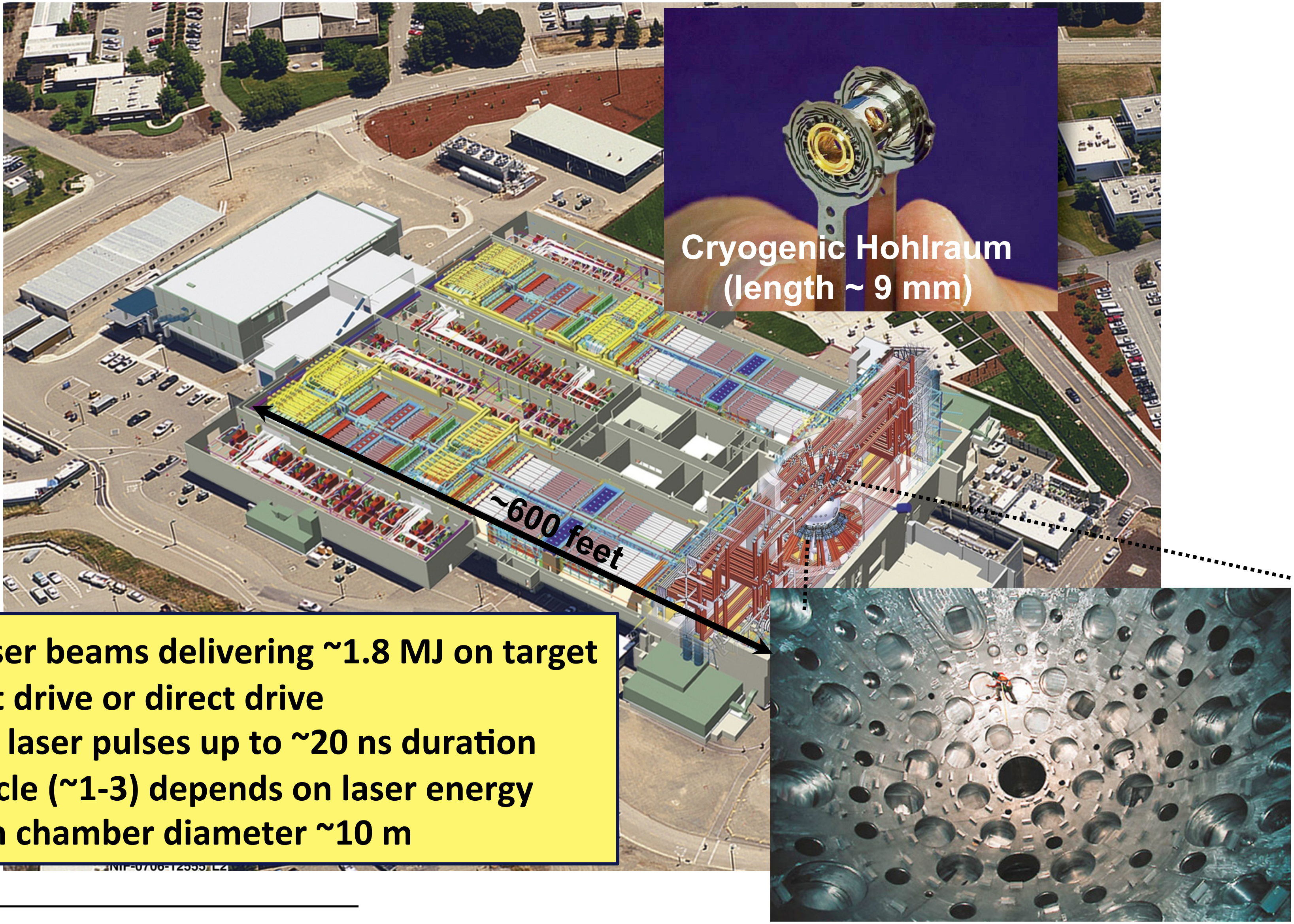

- 192 laser beams delivering ~1.8 MJ on target
- Indirect drive or direct drive
- flexible laser pulses up to ~20 ns duration
- shot cycle (~1-3) depends on laser energy
- vacuum chamber diameter ~10 m

---

*Miller, Nuclear Fusion 44 (2004)

Outline

- High-Energy-Density (HED) Plasma
  - US facilities

Zylstra et al.
(MIT)

- Plasma Nuclear Science using ICF-like implosions
  - p-p chain at relevant Gamow energies

Drake,
Kuranz et al.
(UM)

- Laser-produced Magnetohydrodynamics
  - similarity conditions
  - Rayleigh-Taylor growth in core-collapse SNe

Park,
Huntington et al.
(LLNL)

- Laser-produced Jets
  - ‘collisionless’ shocks
  - supersonic jet dynamics

Manuel,
Kuranz et al.
(UM)

Chen et al.
(LLNL)

- Pair-Plasma Production
  - relativistic jets

- Summary

Inertial fusion utilizes high-power lasers to implode a capsule of DT fuel to ρ~1000 g/cc and T~5 keV

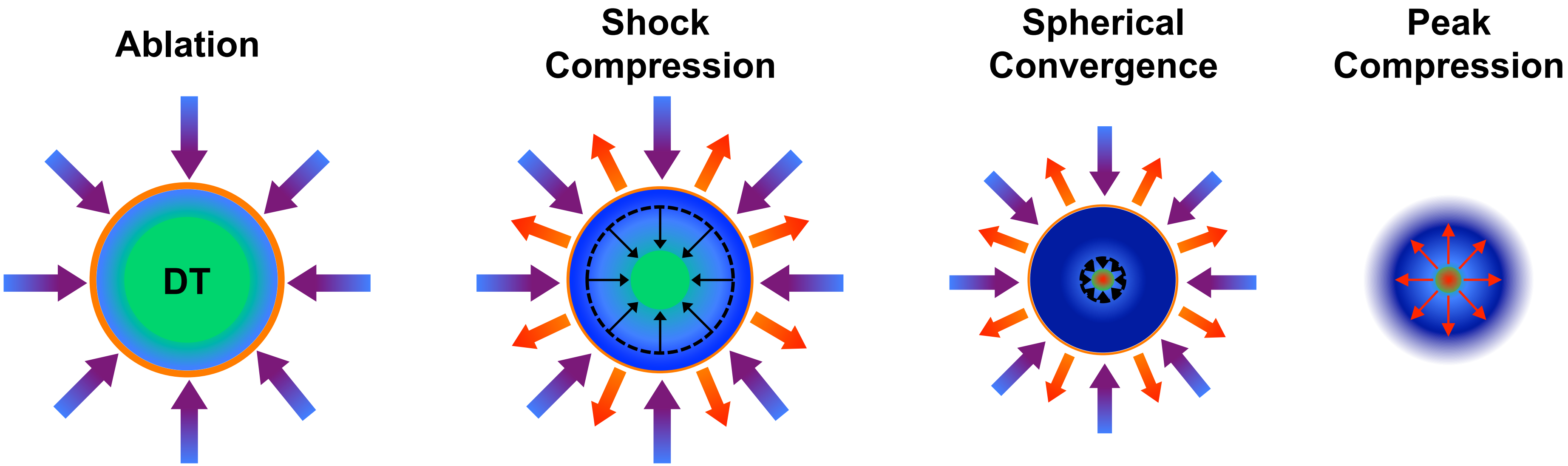

ICF requires precise understanding of many different physics processes:
- laser-plasma interactions
- hydrodynamic instabilities and shock propagation
- nuclear reactions in HED environments
- …

In contrast to accelerators, ICF facilities provide an environment for nuclear reactions in thermalized plasma

Accelerator

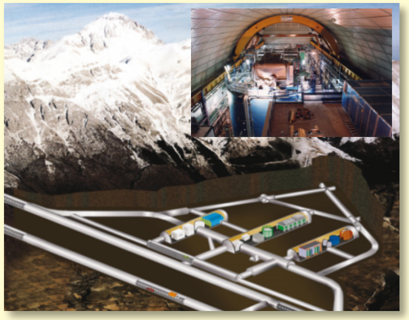

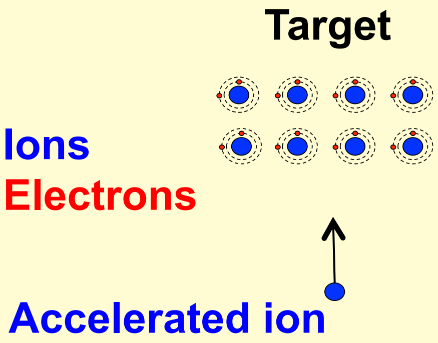

Target

Ions

Electrons

Accelerated ion

- **Monoenergetic beam ions**
- **Bound electron screening**

Plasma

- **Thermal ions**
- **Debye electron screening**

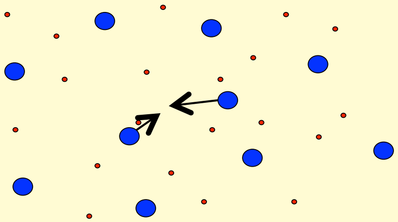

Ions

Electrons

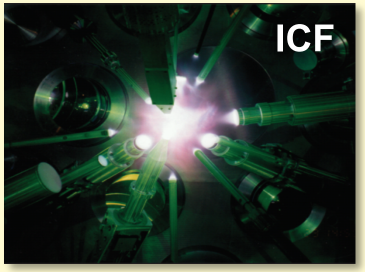

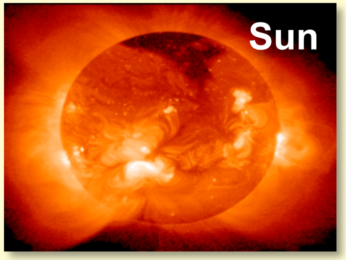

Density:	**0.1 – 1000 g/cc**	**160 g/cc (core)**
Temperature:	**1 – 20 keV**	**1.3 keV (core)**
Mass:	**0.1 µg – 1 mg**	**2×10^{33} g**
Time (s):	**10^{-10} s**	**3×10^{17} s**

---

* M. Aliotta *et al*, NP A (2001), U. Schröder *et al*, NIM B (1989), H. J. Assenbaum *et al*, ZP (1987)

Laser-generated plasmas are created at similar densities and temperatures as those in stellar cores

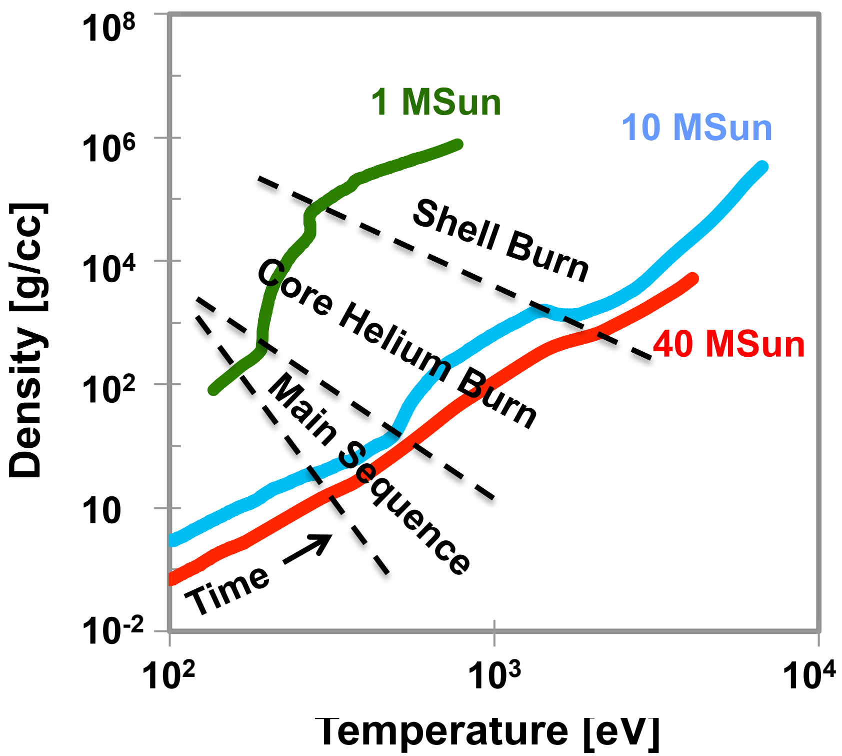

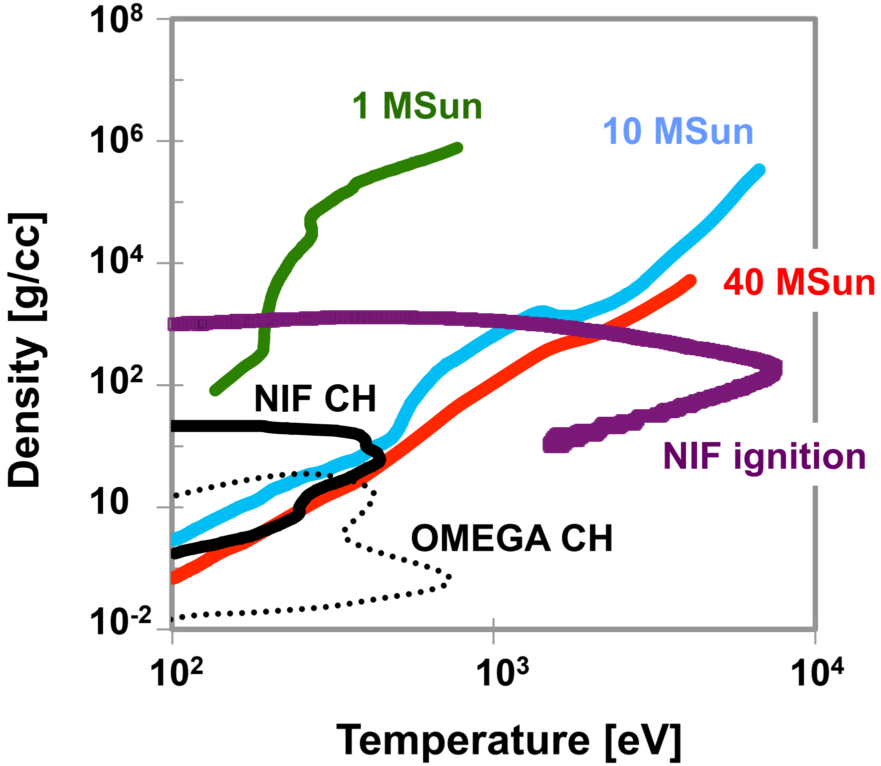

---

* Stellar evolution simulations by Dave Dearborn, NIF Simulations Harry Robey and Bob Tipton, OMEGA Simulation P. B. Radha

The measured ^{3}He+^{3}He proton spectrum displays multiple reaction channels at a Gamow energy of ~165 keV

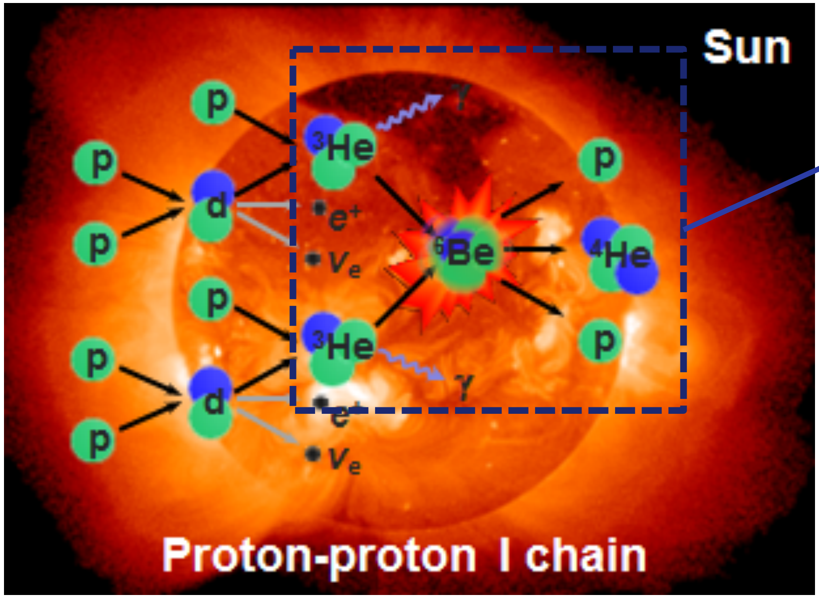

^{3}He + ^{3}He → ^{4}He + 2p (0-10.8 MeV)
→ ^{5}Li + p (9.2 MeV)
→ ^{5}Li* + p

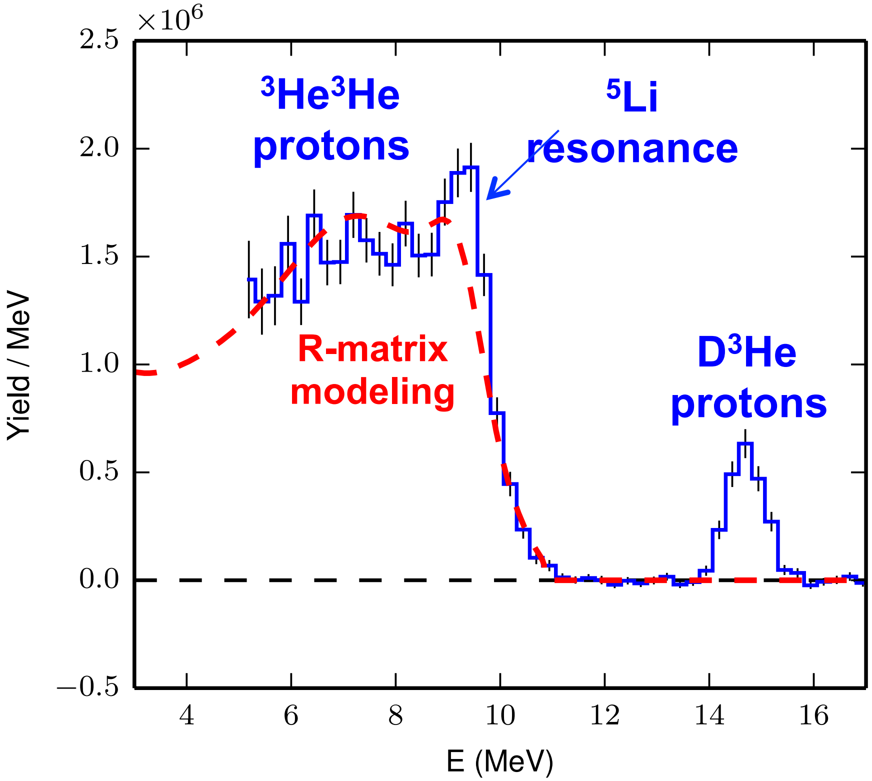

T_i ~ 27 keV
E_G ~ 165 keV
ρ = 0.1 g/cc

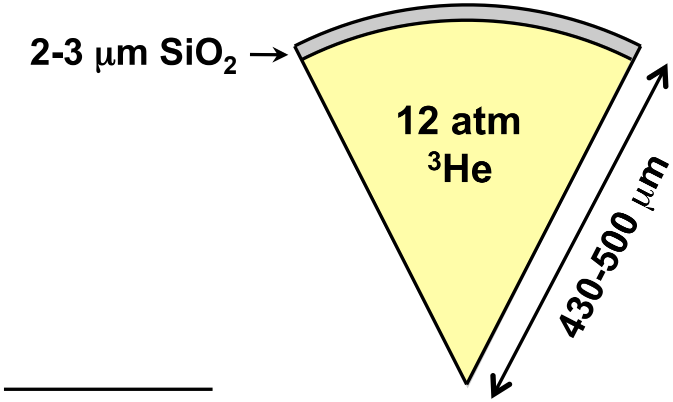

$E_G(^3\text{He}+^3\text{He}) \approx 18.1 \times Ti^{0.67}$ [keV]

Recent experiments implemented a Gamma Cerenkov Detector (GCD) to measure D+p 5.5 MeV γ-rays

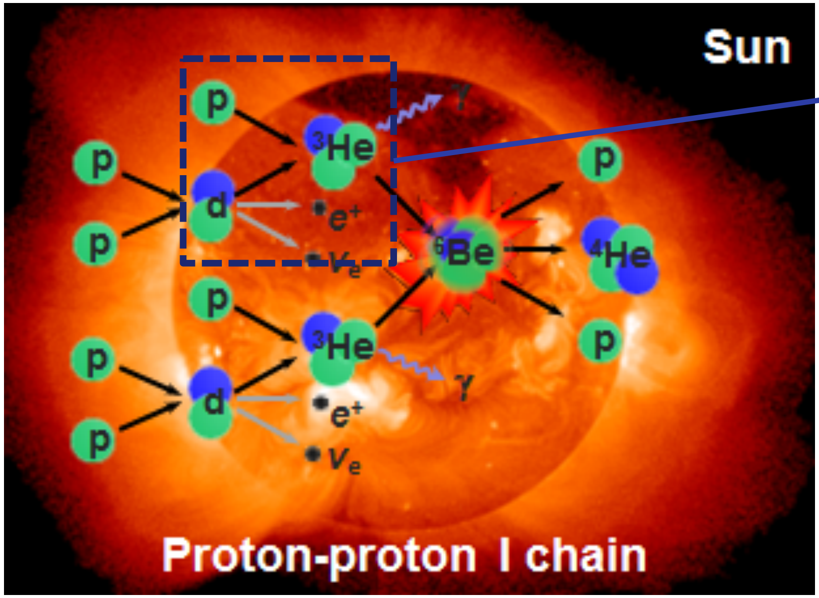

T_i ~ 5-12 keV
E_G ~ 10-30 keV

$D + p \rightarrow {}^3He + \gamma$ (5.5 MeV)

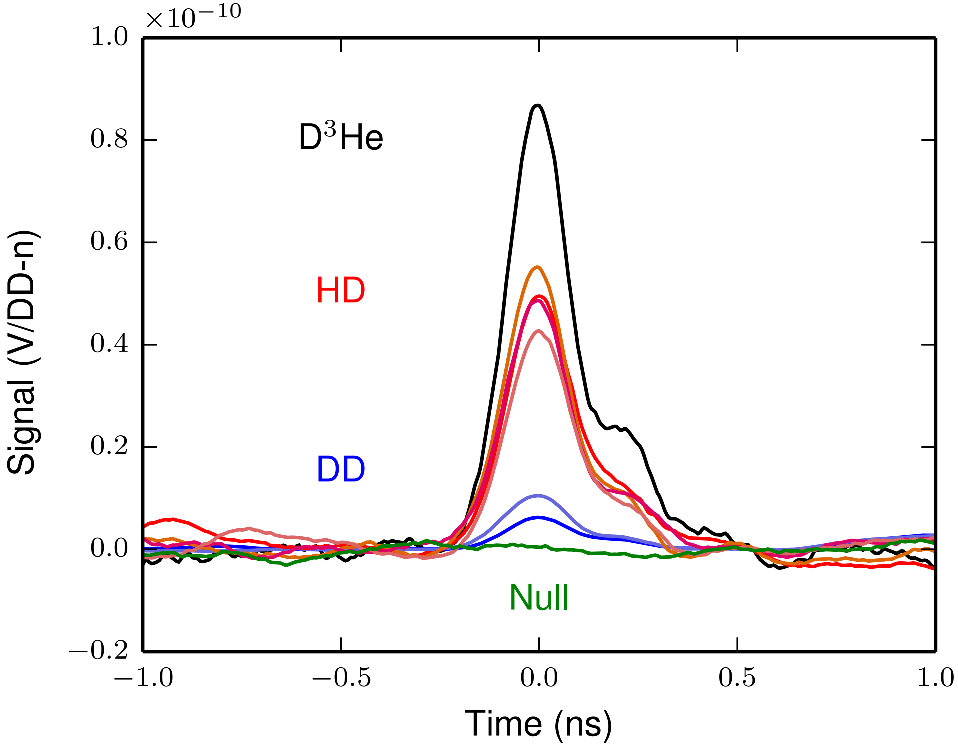

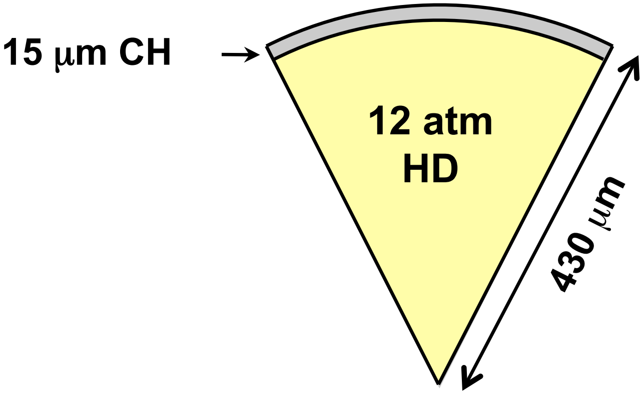

Precise understanding of this reaction at low Gamow energy is important for protostars and brown dwarfs.

There is a rich set of opportunities to study nuclear reactions at OMEGA and the NIF

Current work

Charged-particle induced reactions:

- **T(t,2n)^{4}He** (analogue to ^{3}He(^{3}He,2p)^{4}He).
- **T(^{3}He,np)^{4}He, T(^{3}He,d) ^{4}He, T(^{3}He,γ)^{6}Li** (impact BBN?).
- **^{3}He(^{3}He,2p)^{4}He** (pp-I).
- **D(p,γ)^{3}He** (Brown dwarfs, protostars).
- **^{6}Li(p,α)^{3}He**
- **^{7}Li(p,α)^{4}He**
- **^{7}Be(p,γ)^{8}B** (pp-III).
- **^{11}B(p,α)^{8}Be** (non-Maxwellian ion distributions).
- **^{15}N(p,α)^{12}C** (last step of CNO).
- **^{12}C(α,γ)^{16}O** ?

Neutron-induced reactions:

- **n-d and n-T** at 14 MeV
- **D(n,2n)** at 14 MeV
- **T(n,2n)** at 14 MeV
- Various (n,γ), (n,2n) processes?

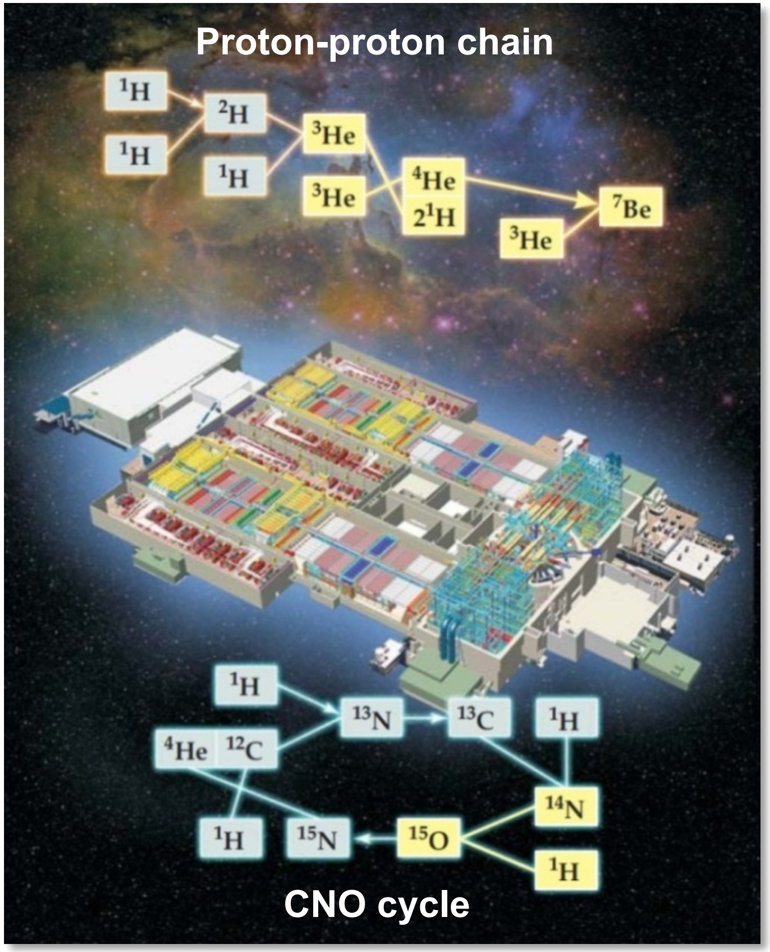

Outline

- ➢ High-Energy-Density (HED) Plasma
  - US facilities

Zylstra et al.
(MIT)

- ➢ Plasma Nuclear Science using ICF-like implosions
  - p-p chain at relevant Gamow energies

Drake,
Kuranz et al.
(UM)

- ➢ Laser-produced Magnetohydrodynamics
  - similarity conditions
  - Rayleigh-Taylor growth in core-collapse SNe

Park,
Huntington et al.
(LLNL)

Manuel,
Kuranz et al.
(UM)

- ➢ Laser-produced Jets
  - ‘collisionless’ shocks
  - supersonic jet dynamics

Chen et al.
(LLNL)

- ➢ Pair-Plasma Production
  - relativistic jets

- ➢ Summary

Magnetohydrodynamic (MHD) equations describe both laboratory and astrophysical systems

Continuity

$$\frac{\partial \rho}{\partial t} + \nabla \cdot \rho \mathbf{v} = 0$$

Momentum

$$\rho \left(\frac{\partial \mathbf{v}}{\partial t} + \mathbf{v} \cdot \nabla \mathbf{v} \right) = -\nabla p + \frac{1}{\mu_0} \left(\nabla \times \mathbf{B} \right) \times \mathbf{B}$$

Energy

$$\frac{\partial p}{\partial t} - \gamma \frac{p}{\rho} \frac{\partial \rho}{\partial t} + \mathbf{v} \cdot \nabla p - \gamma \frac{p}{\rho} \mathbf{v} \cdot \nabla \rho = 0$$

Field Evolution

$$\frac{\partial \mathbf{B}}{\partial t} = \nabla \times \left(\mathbf{v} \times \mathbf{B} \right)$$

---

[1] Ryutov, ApJ 518 (1999)
[2] Ryutov, POP 8 (2001)
[3] Drake, High-energy-density physics (2006), ch 10
[4] Remington, RMP 78 (2006)
[5] Falize, ApJ 730 (2011)

Multiple dimensionless parameters determine the validity of using the MHD equations to describe system dynamics

- **The system exhibits fluid-like behavior** $l_{mfp}/L << 1$
- **Energy flow by particle heat conduction is negligible** $\mathrm{Pe} >> 1$
- **Energy flow by radiation flux is negligible** $\mathrm{Pe}_{\gamma} >> 1$
- **Viscous dissipation is negligible** $\mathrm{Re} >> 1$

Astrophysical systems are large and fulfill these criteria in many cases!

Multiple dimensionless parameters determine the validity of using the MHD equations to describe system dynamics

Parameter	SN	Lab
l_{mfp}/L	4×10^{-3}	4×10^{-9}
Pe	1.1×10^{13}	5.9×10^{3}
Pe_{γ}	1.6×10^{16}	1.6×10^{10}
Re	1.9×10^{11}	1.4×10^{5}

$l_{mfp}/L << 1$

$\mathrm{Pe} >> 1$

$\mathrm{Pe}_{\gamma} >> 1$

$\mathrm{Re} >> 1$

Two MHD systems evolve similarly when the Euler number (Eu) and magnetization (μ) are similar.

$$\mathrm{Eu} \equiv \frac{v^*}{\sqrt{p^*/\rho^*}} \qquad \mu \equiv \frac{\left(B^*\right)^2}{p^*}$$

---

* Drake, ApJ 564 (2002) Table 1

Outline

- High-Energy-Density (HED) Plasma
  - US facilities

Zylstra et al.
(MIT)

- Plasma Nuclear Science using ICF-like implosions
  - p-p chain at relevant Gamow energies

Drake,
Kuranz et al.
(UM)

- Laser-produced Magnetohydrodynamics
  - similarity conditions
  - Rayleigh-Taylor growth in core-collapse SNe

Park,
Huntington et al.
(LLNL)

- Laser-produced Jets
  - ‘collisionless’ shocks
  - supersonic jet dynamics

Manuel,
Kuranz et al.
(UM)

Chen et al.
(LLNL)

- Pair-Plasma Production
  - relativistic jets

- Summary

SN1987a stimulated research into Rayleigh-Taylor growth in supernovae explosions

SN1987A, Hubble Space Telescope

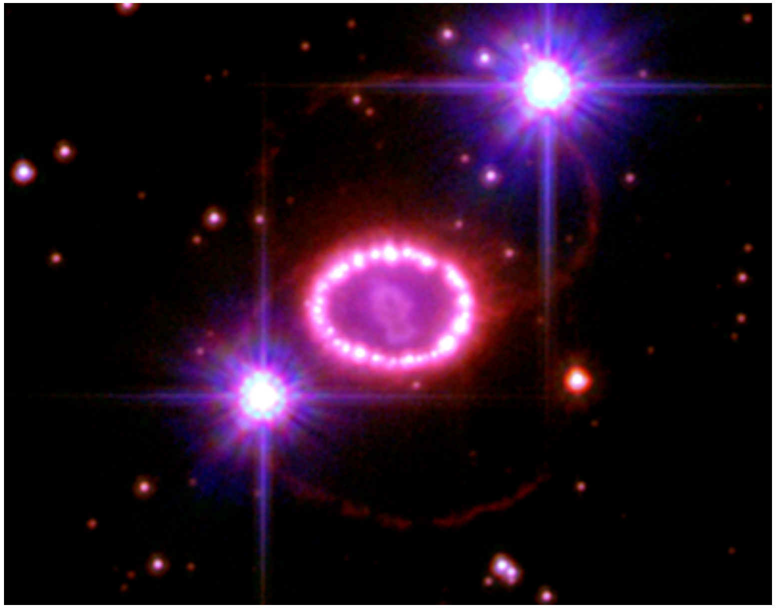

- Core-collapse supernova of a bluegiant
- Light curve data suggested* ‘mixing’ between stellar layers

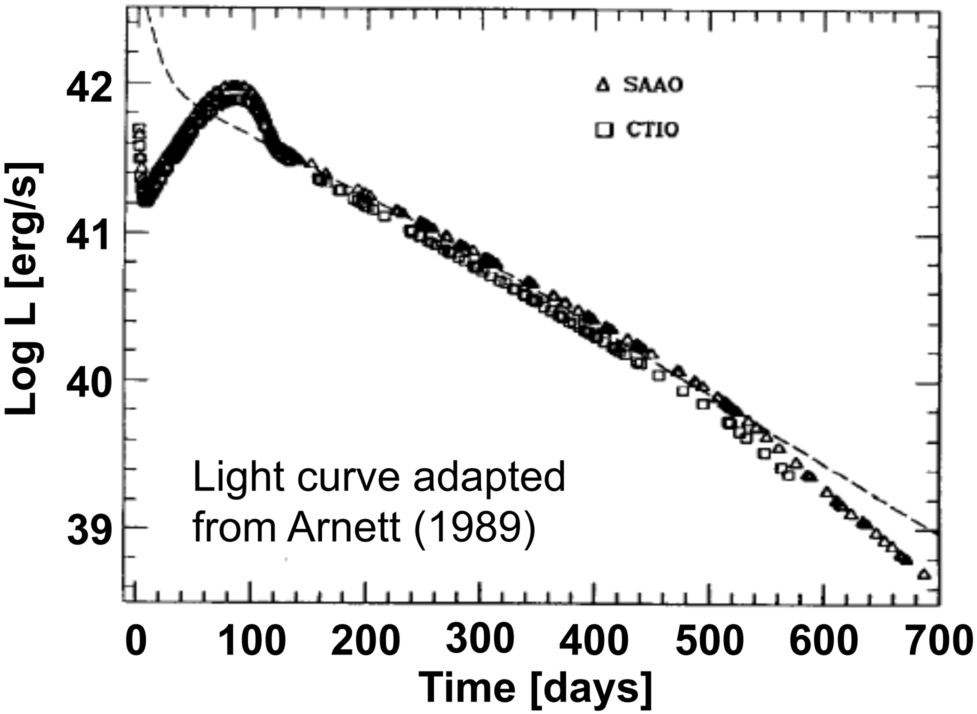

Light curve adapted from Arnett (1989)

Can mixing in supernovae be investigated in the lab?

---

* Arnett, ARAA 27 (1989)

Simulations suggest that geometric similarities are sufficient to investigate instability growth in SNe

1D PROMETHEUS simulation
He-H interface in SN1987a

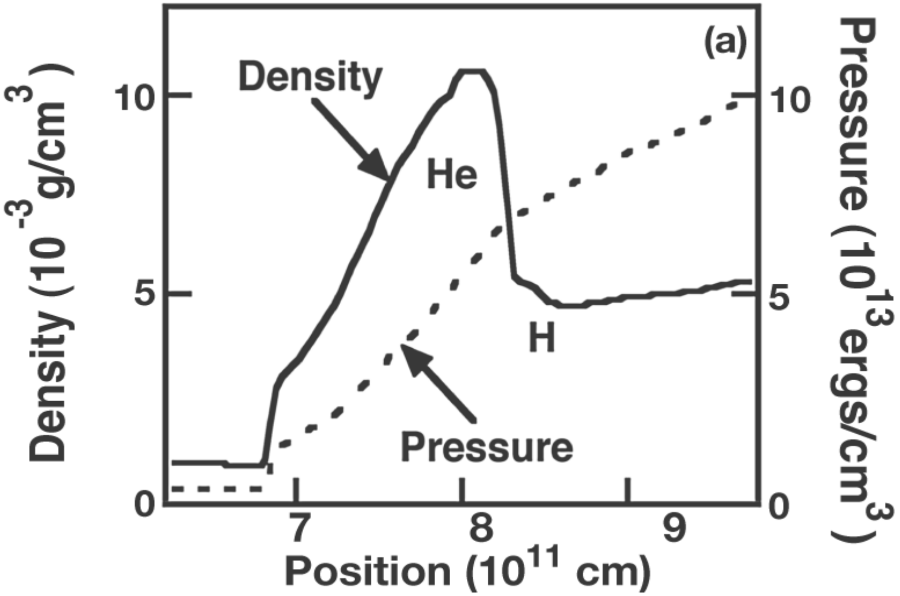

1D HYADES simulation
OMEGA experiment

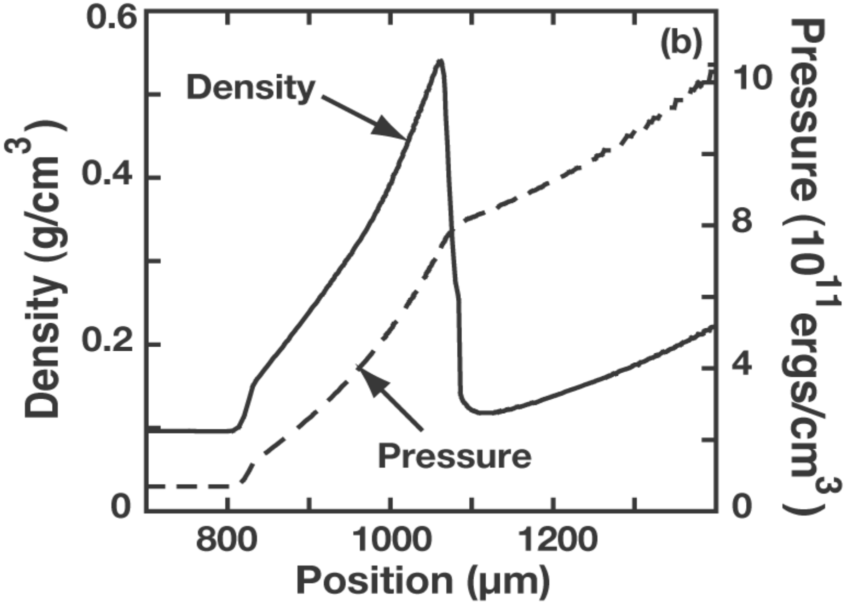

The Euler number is approximately equal between the two systems.

$$\mathrm{Eu}_{SN} \approx 2.2 \qquad \mathrm{Eu}_{Exp} \approx 2.3$$

---

* Kuranz, ApJ 696 (2009) Fig. 1

Simulations demonstrate the similarity of the interface-velocity evolution in both systems

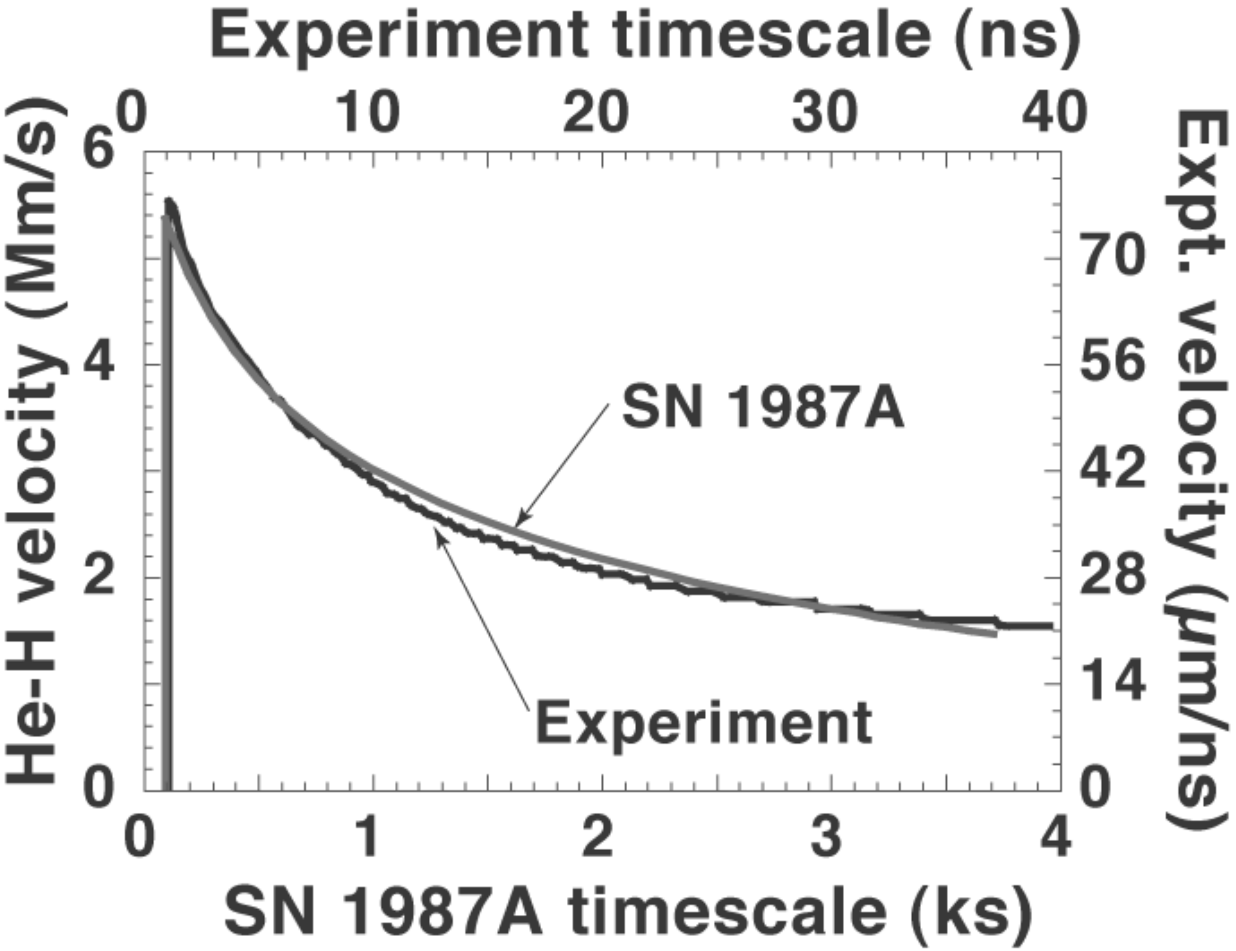

---

* Kuranz, ApJ 696 (2009) Fig. 1

Scaled experiments investigated instability growth at the He-H interface in supernovae

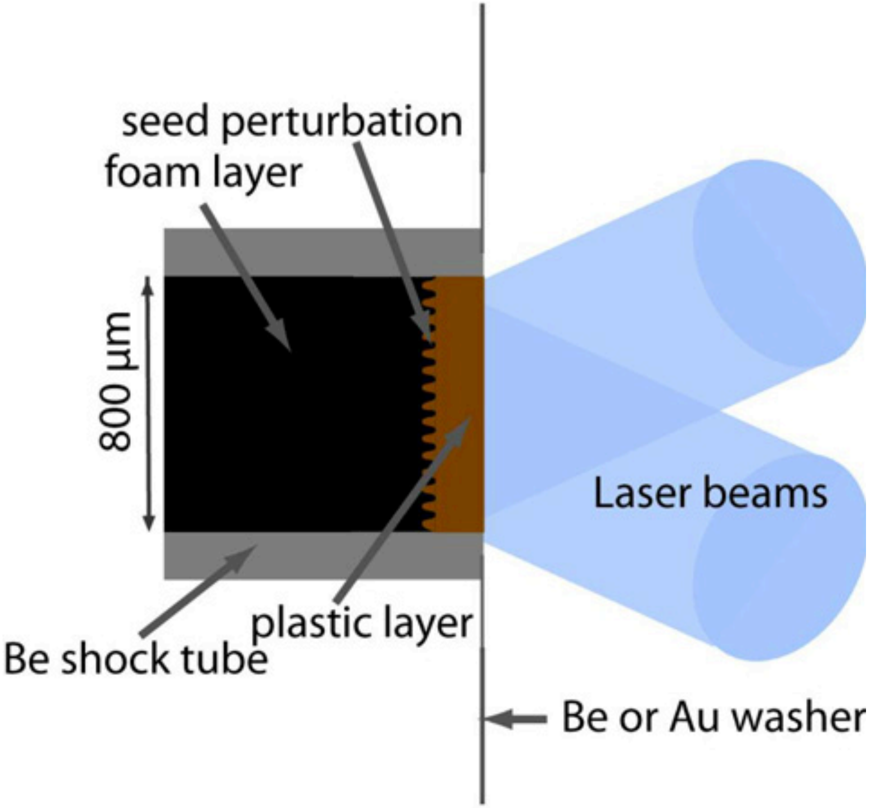

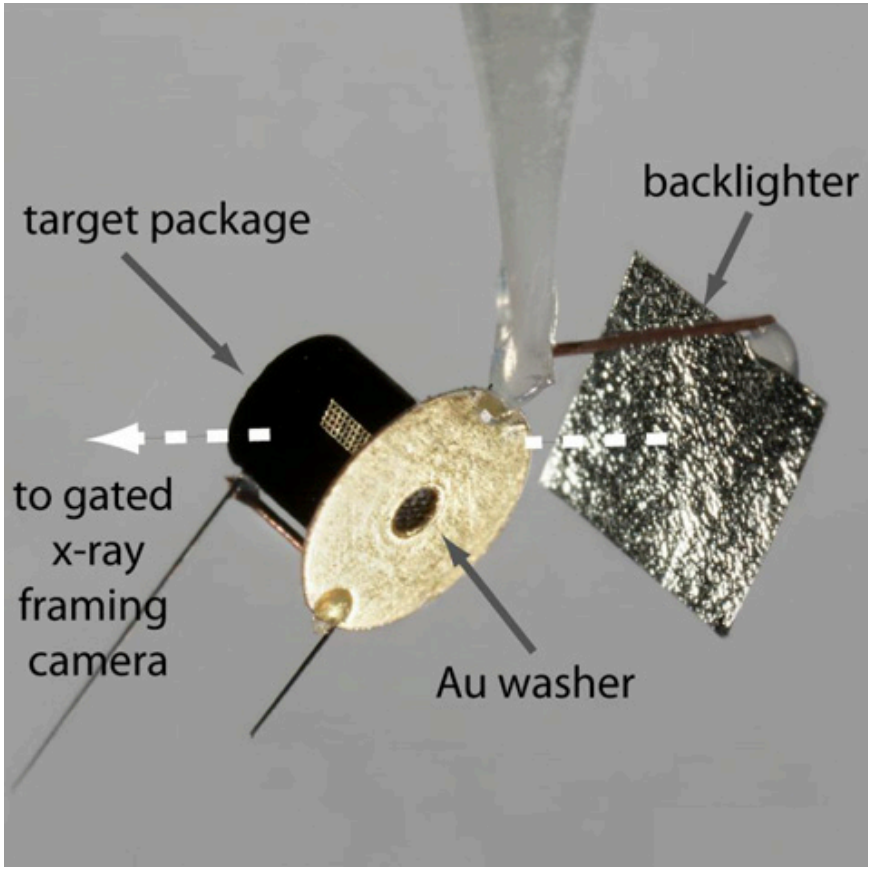

---

* Kuranz, ApJ 696 (2009) Fig. 2

Scaled experiments investigated instability growth at the He-H interface in supernovae

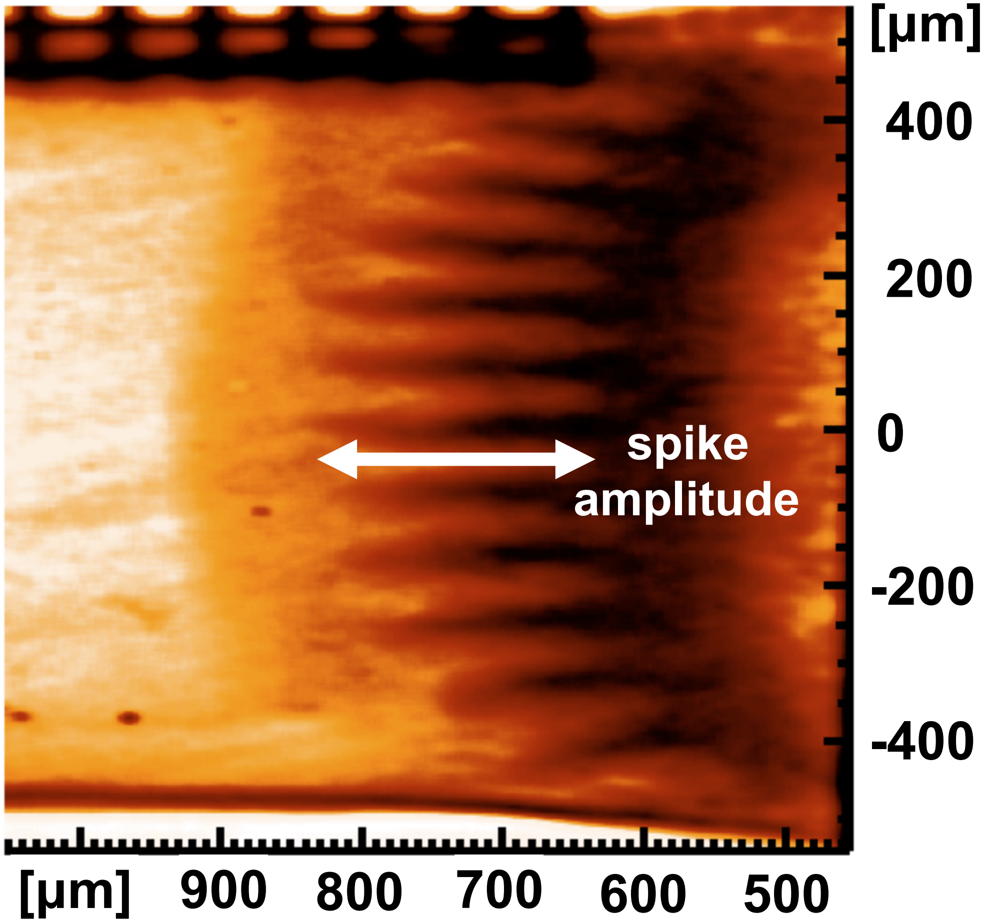

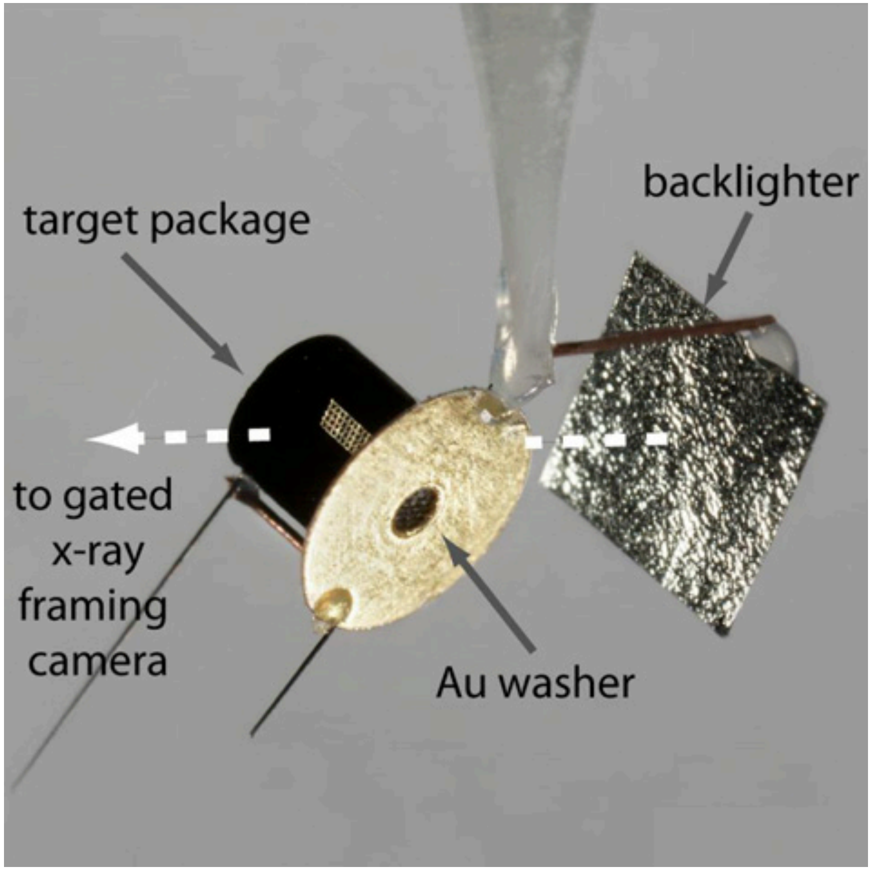

X-ray radiographs demonstrated that amplitude growth was consistent with the nonlinear 'buoyancy-drag' model.

---

* Kuranz, POP 16 (2009) Fig. 5

Scaled experiments investigated instability growth at the He-H interface in supernovae

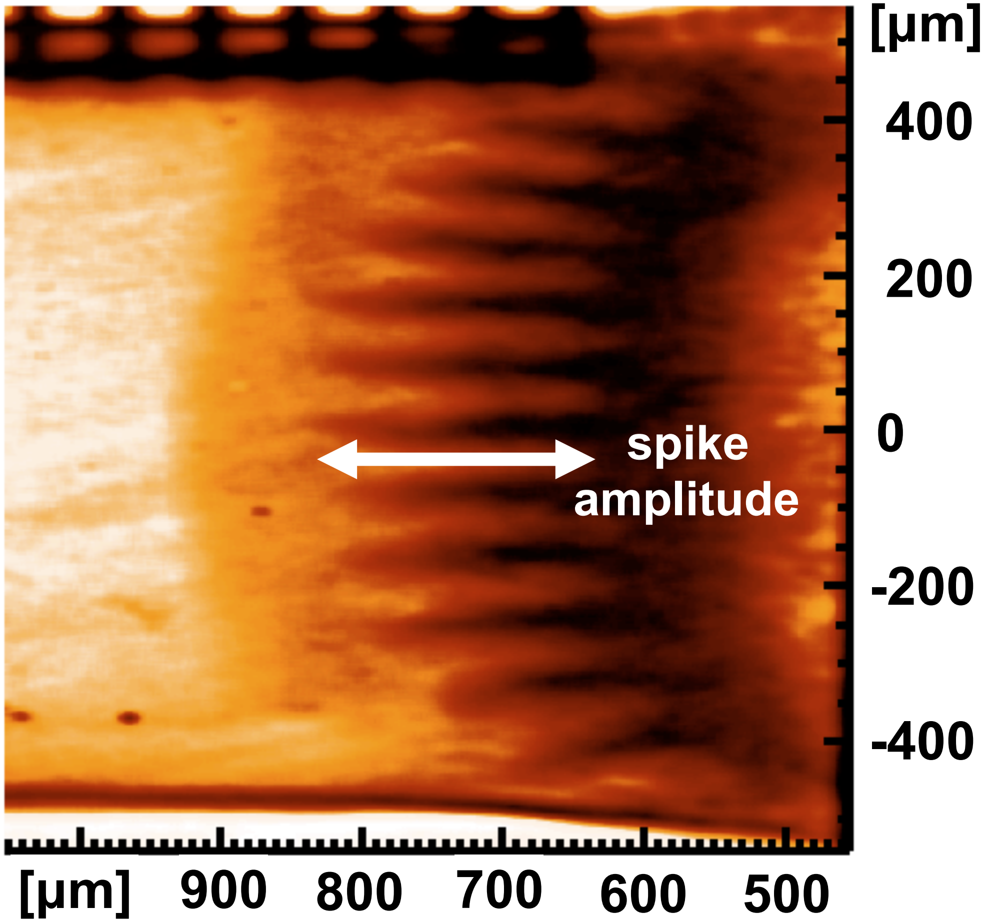

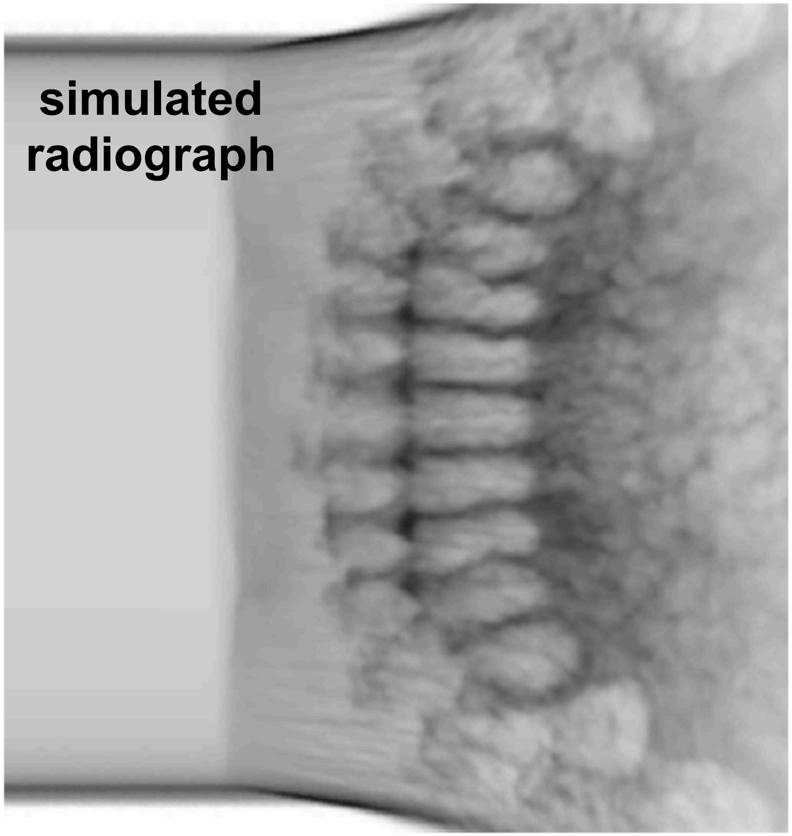

… but the detailed spike morphology is different!

---

* Kuranz, POP 16 (2009) Fig. 5; Kuranz POP 17 (2010) Fig. 8

Outline

- High-Energy-Density (HED) Plasma
  - US facilities

Zylstra et al.
(MIT)

- Plasma Nuclear Science using ICF-like implosions
  - p-p chain at relevant Gamow energies

Drake,
Kuranz et al.
(UM)

- Laser-produced Magnetohydrodynamics
  - similarity conditions
  - Rayleigh-Taylor growth in core-collapse SNe

Park,
Huntington et al.
(LLNL)

- Laser-produced Jets
  - ‘collisionless’ shocks
  - supersonic jet dynamics

Manuel,
Kuranz et al.
(UM)

Chen et al.
(LLNL)

- Pair-Plasma Production
  - relativistic jets

- Summary

Shocks are formed in many astrophysical objects, but how are 'collisionless' shocks created

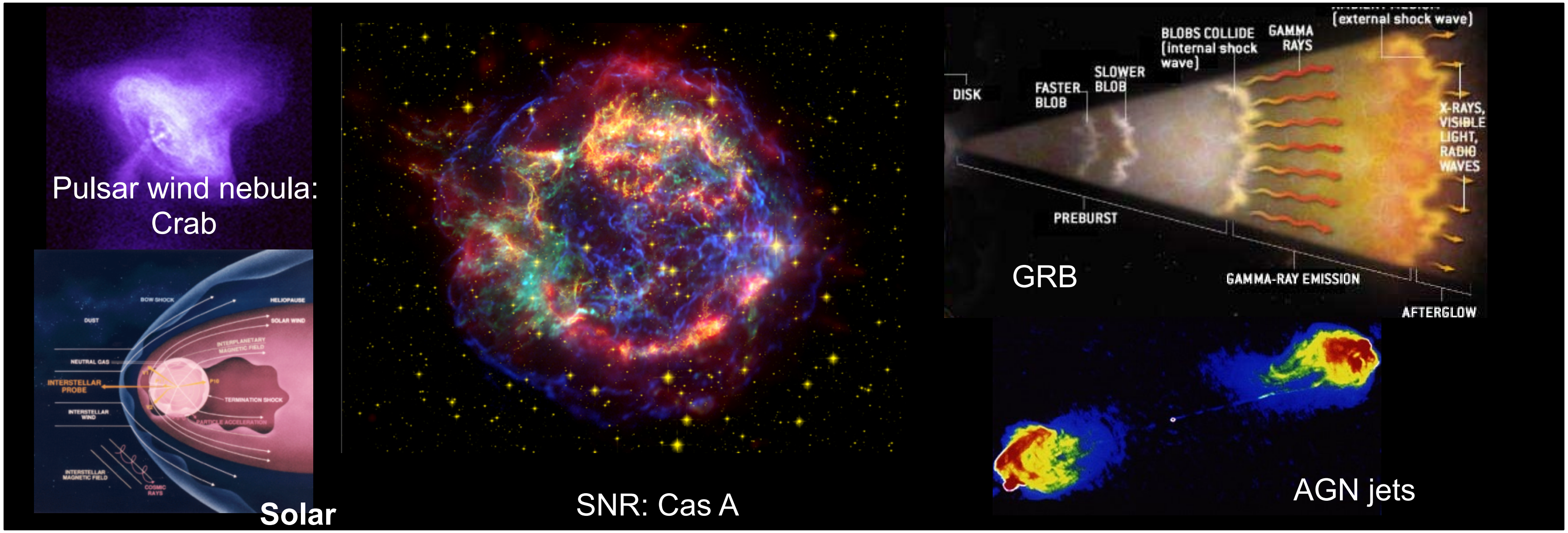

Pulsar wind nebula: Crab

Solar

SNR: Cas A

GRB

AGN jets

- **Shocks are typically created through the pile-up of pressure waves through collisions with a thickness ~λ_{mfp}**
- **In many astrophysical objects, λ_{mfp} >> scales of interest**
- **Some observed shocks are 'collisionless'…**

Collisionless shocks are mediated through scattering events with magnetic fields

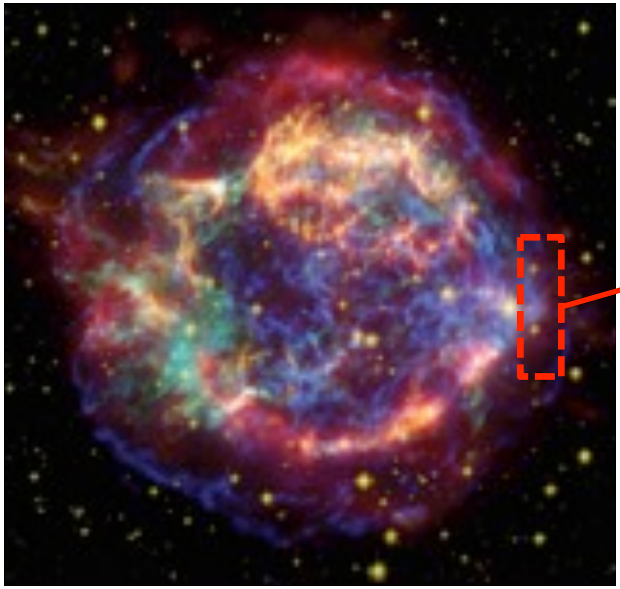

SNR Cassiopeia A

Collisionless plasma flows

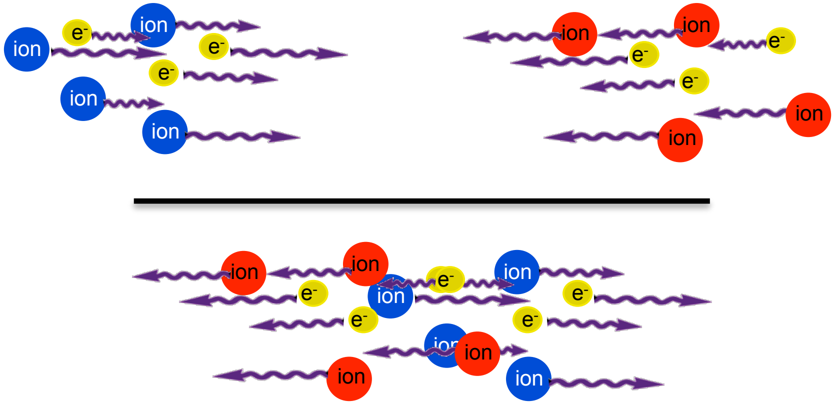

Do ions pass through without creating a shock?

Strong (scattering) fields may be self-generated or be created through compression of preexisting background fields.

Numerical modeling suggests that both scattering mechanisms may produce shocks

self-generated magnetic fields (filamentation/Weibel instability)

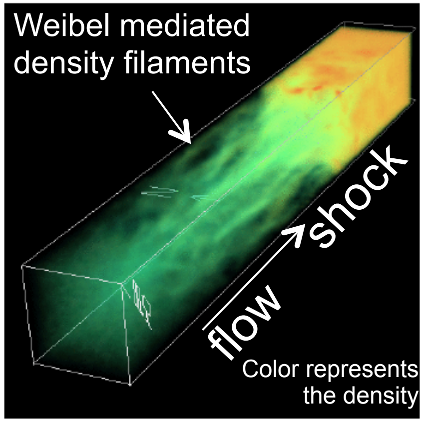

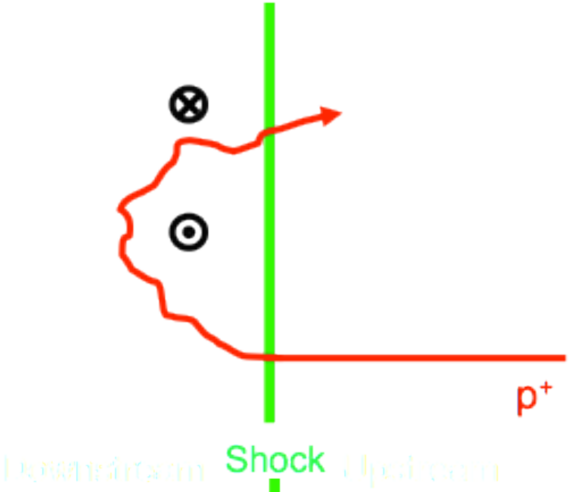

Compressed pre-existing fields

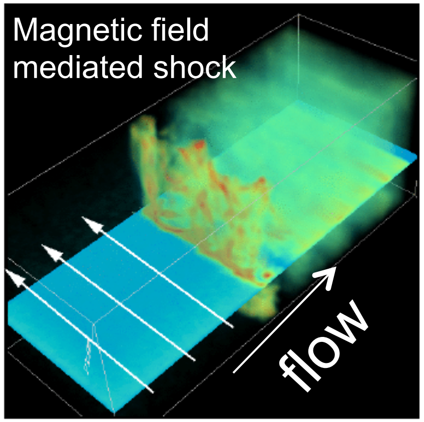

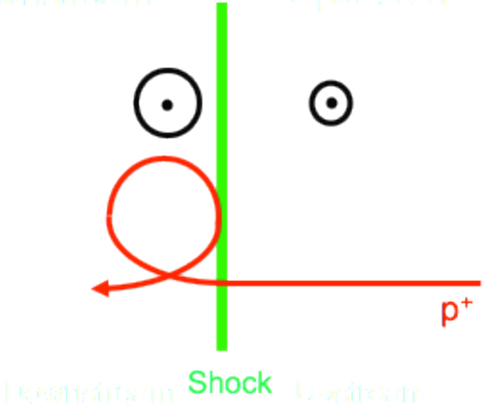

Simulations suggest that self-generated B-fields can mediate shocks over long scale lengths (>100 c/ω_{pi})

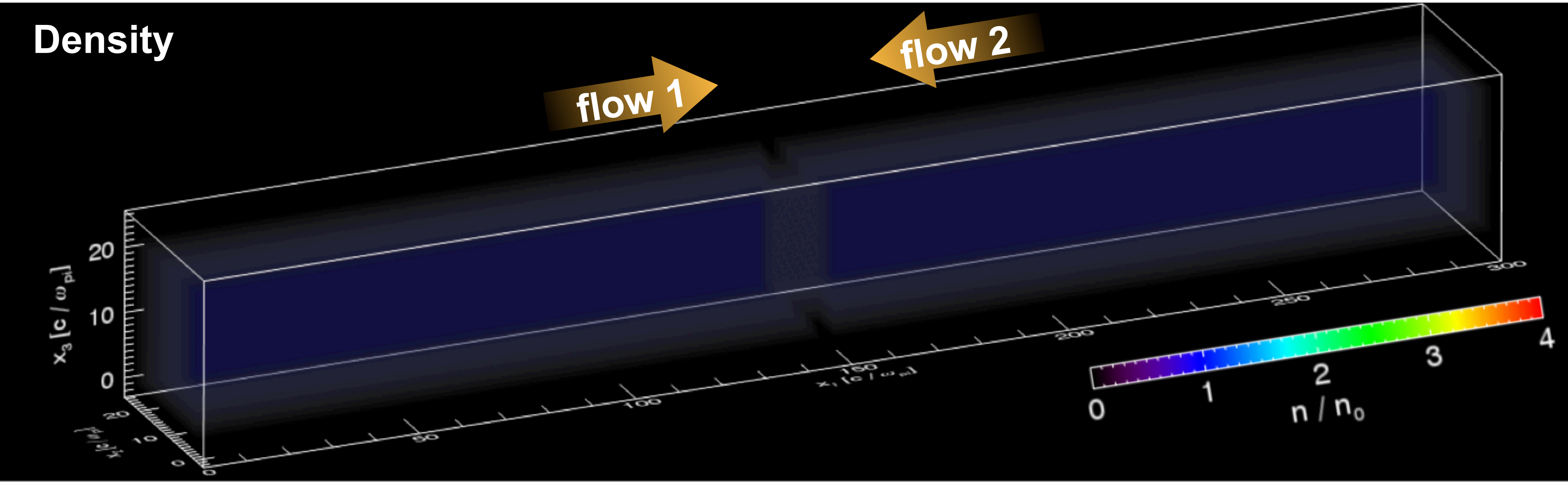

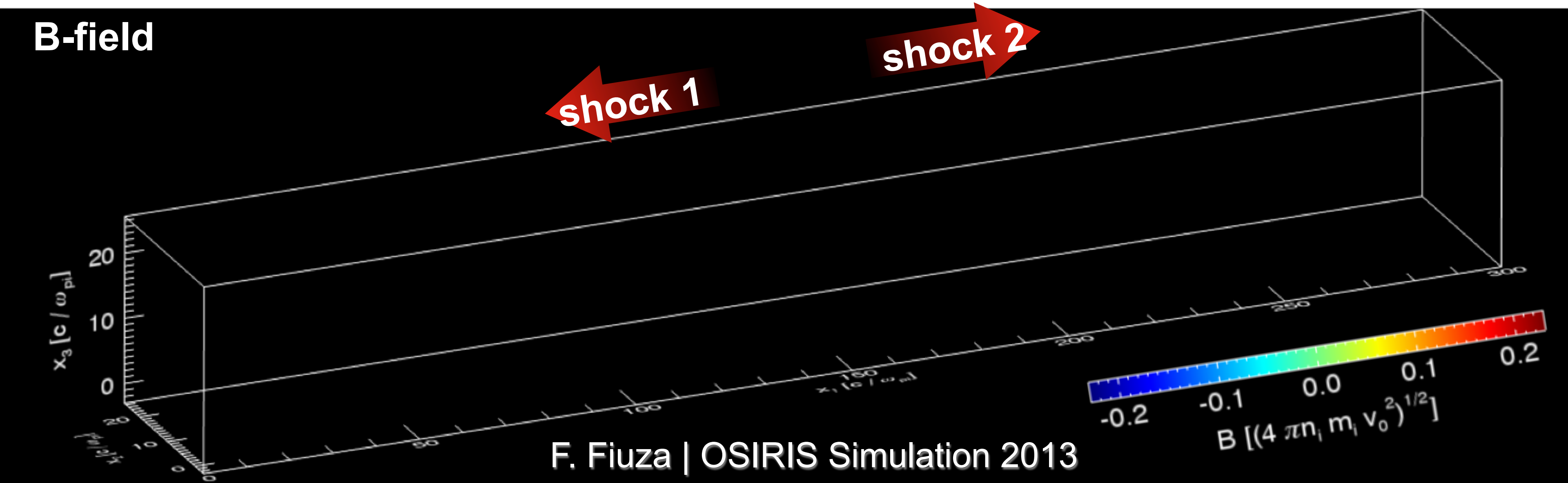

F. Fiuza | OSIRIS Simulation 2013

Proton imaging reproducibly shows self-organized B-fields in collisionless counter-streaming plasmas

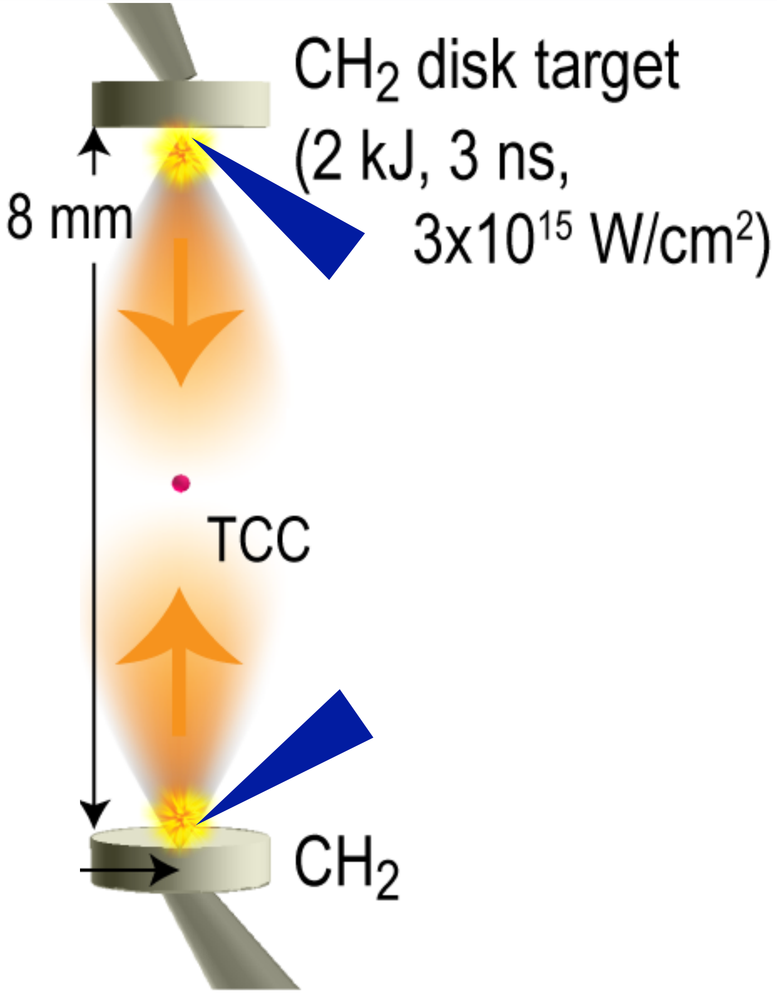

Proton imaging reproducibly shows self-organized B-fields in collisionless counter-streaming plasmas

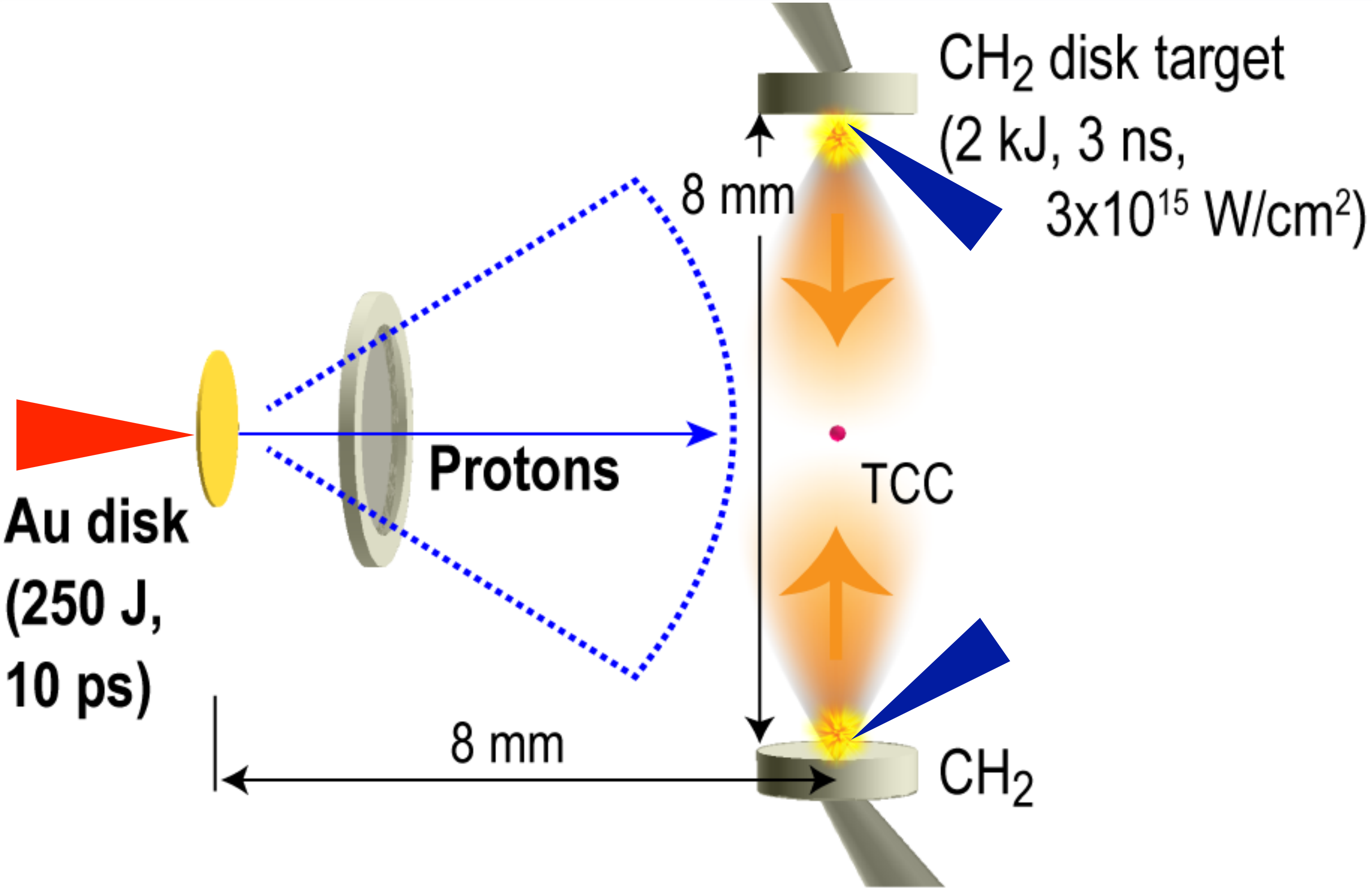

Proton imaging reproducibly shows self-organized B-fields in collisionless counter-streaming plasmas

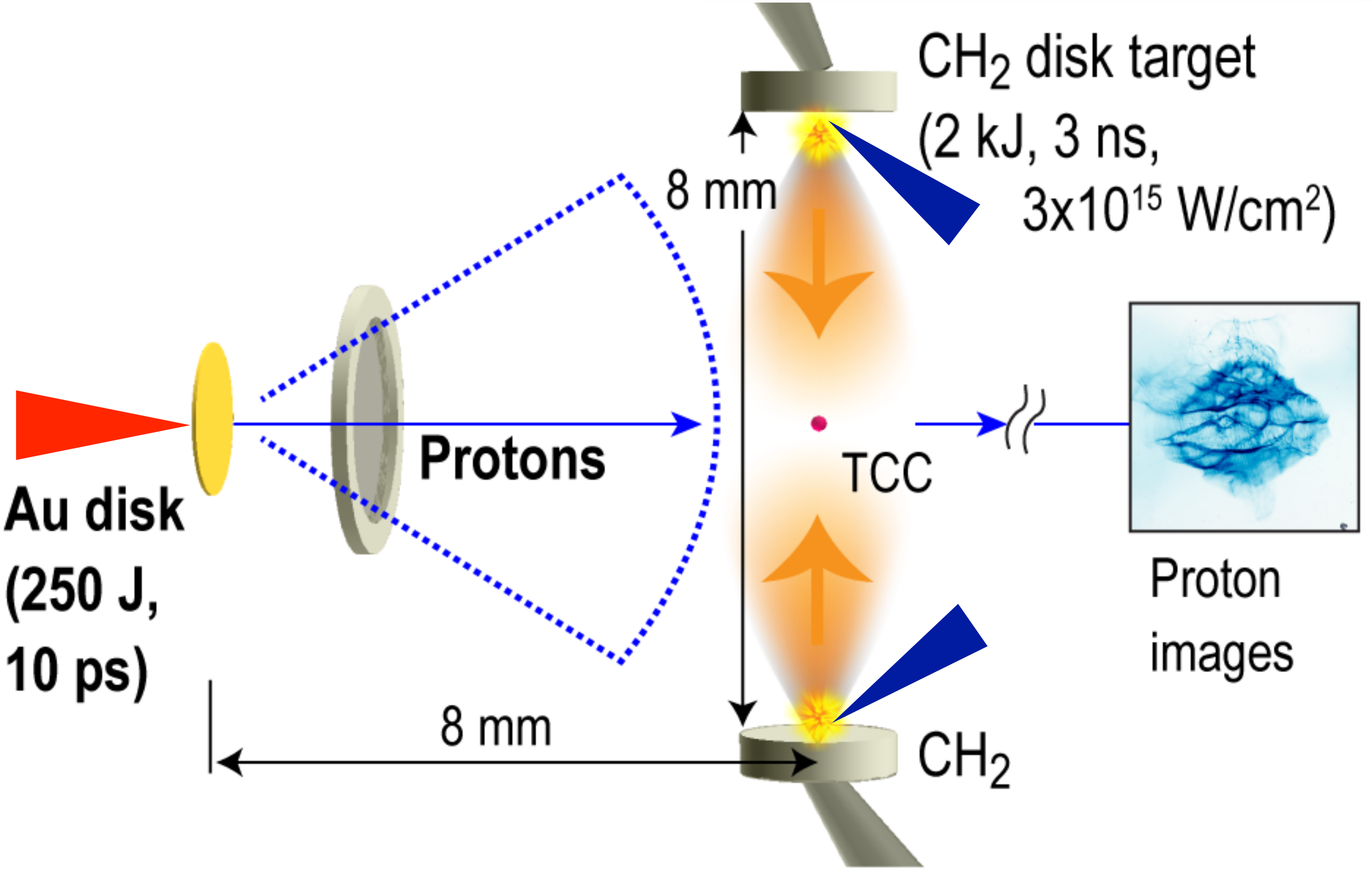

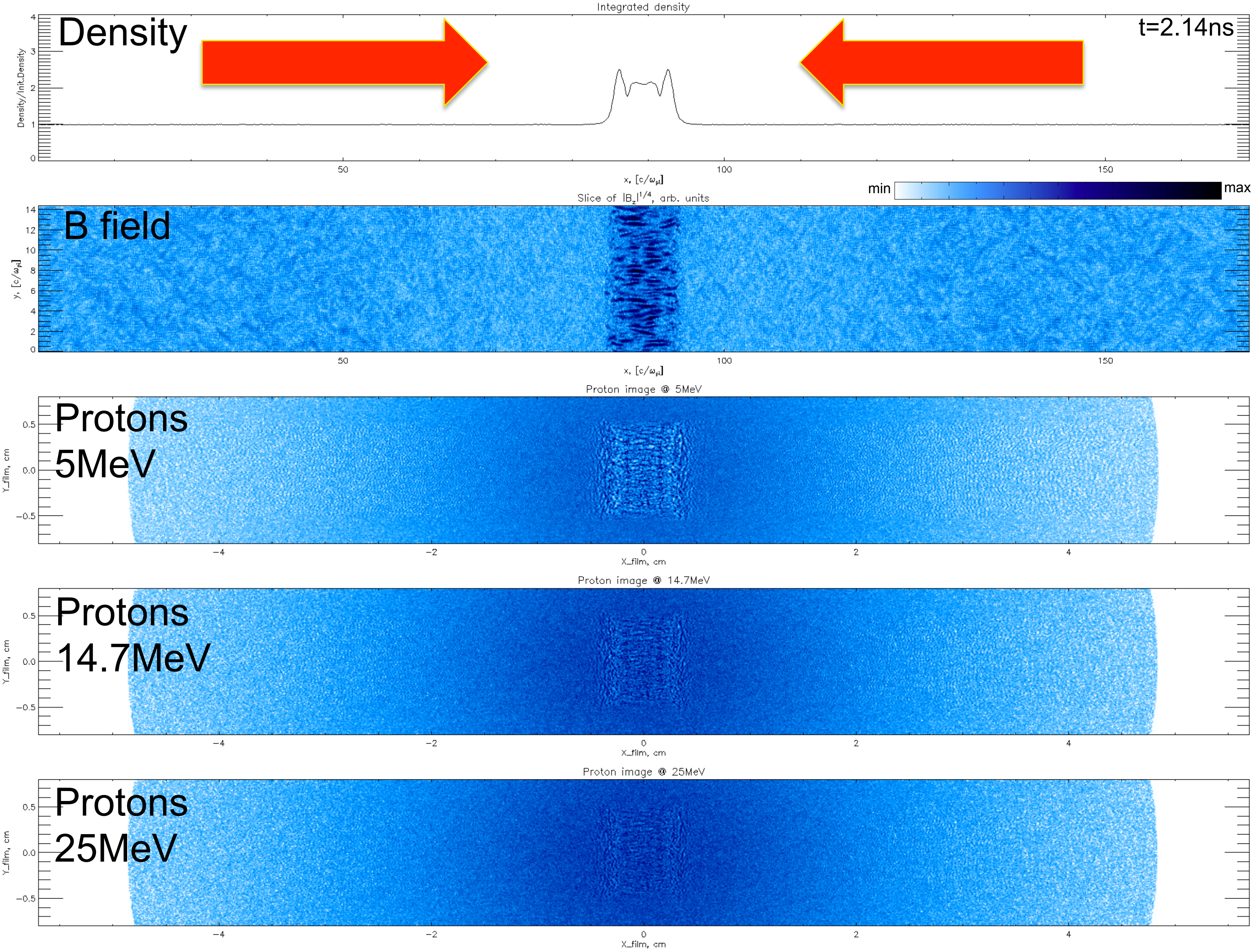
Integrated density
Density
t=2.14ns
Density/Init.Density
0
1
2
3
4
50
100
150
x, [c/ωpl]
Slice of |Bz|^1/4, arb. units
min
max
B field
y, [c/ωpl]
0
2
4
6
8
10
12
14
50
100
150
x, [c/ωpl]
Proton image @ 5MeV
Protons 5MeV
Y_film, cm
0.5
0.0
−0.5
−4
−2
0
2
4
X_film, cm
Proton image @ 14.7MeV
Protons 14.7MeV
Y_film, cm
0.5
0.0
−0.5
−4
−2
0
2
4
X_film, cm
Proton image @ 25MeV
Protons 25MeV
Y_film, cm
0.5
0.0
−0.5
−4
−2
0
2
4
X_film, cm

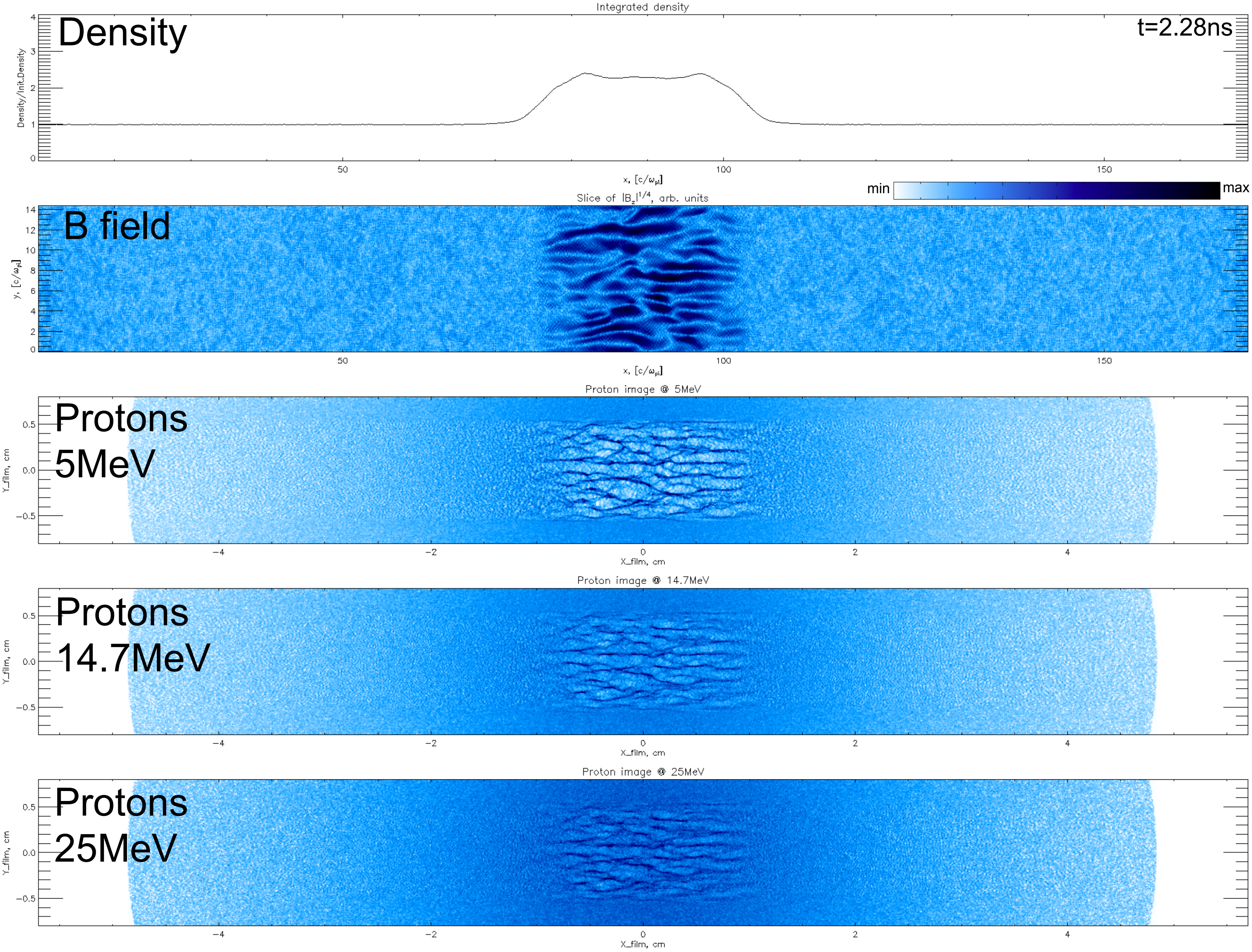
Integrated density
Density
t=2.28ns
Density/Init.Density
0
1
2
3
4
50
100
150
x, [c/ω_{pi}]
min
max
Slice of $|B_z|^{1/4}$, arb. units
B field
y, [c/ω_{pi}]
0
2
4
6
8
10
12
14
50
100
150
x, [c/ω_{pi}]
Proton image @ 5MeV
Protons
5MeV
Y_film, cm
0.5
0.0
−0.5
−4
−2
0
2
4
X_film, cm
Proton image @ 14.7MeV
Protons
14.7MeV
Y_film, cm
0.5
0.0
−0.5
−4
−2
0
2
4
X_film, cm
Proton image @ 25MeV
Protons
25MeV
Y_film, cm
0.5
0.0
−0.5
−4
−2
0
2
4
X_film, cm

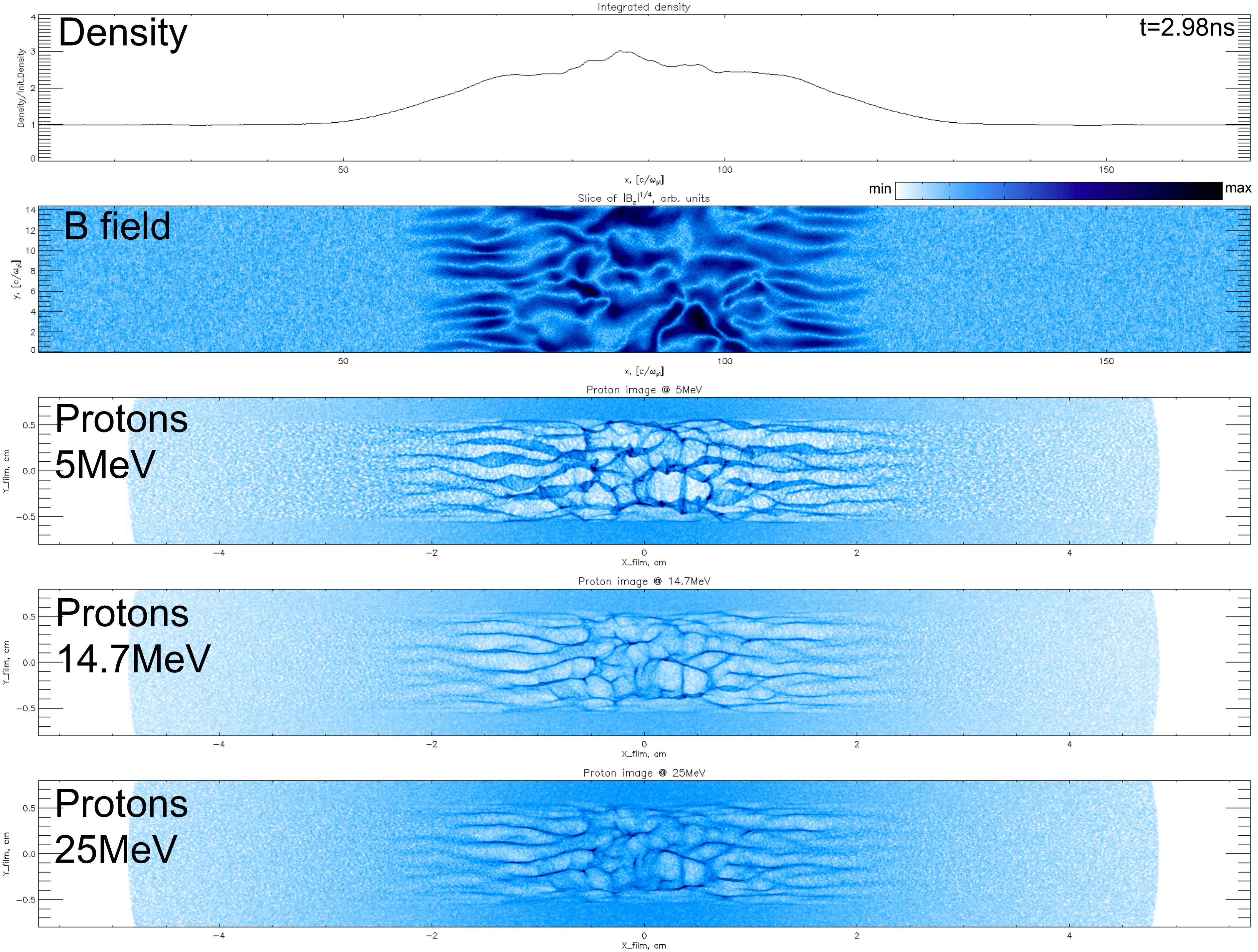
Integrated density
Density
t=2.98ns
Density/Init.Density
0
1
2
3
4
50
100
150
x, [c/ω_pi]
Slice of |B_z|^1/4, arb. units
min
max
B field
y, [c/ω_pi]
0
2
4
6
8
10
12
14
50
100
150
x, [c/ω_pi]
Proton image @ 5MeV
Protons
5MeV
Y_film, cm
0.5
0.0
−0.5
−4
−2
0
2
4
X_film, cm
Proton image @ 14.7MeV
Protons
14.7MeV
Y_film, cm
0.5
0.0
−0.5
−4
−2
0
2
4
X_film, cm
Proton image @ 25MeV
Protons
25MeV
Y_film, cm
0.5
0.0
−0.5
−4
−2
0
2
4
X_film, cm

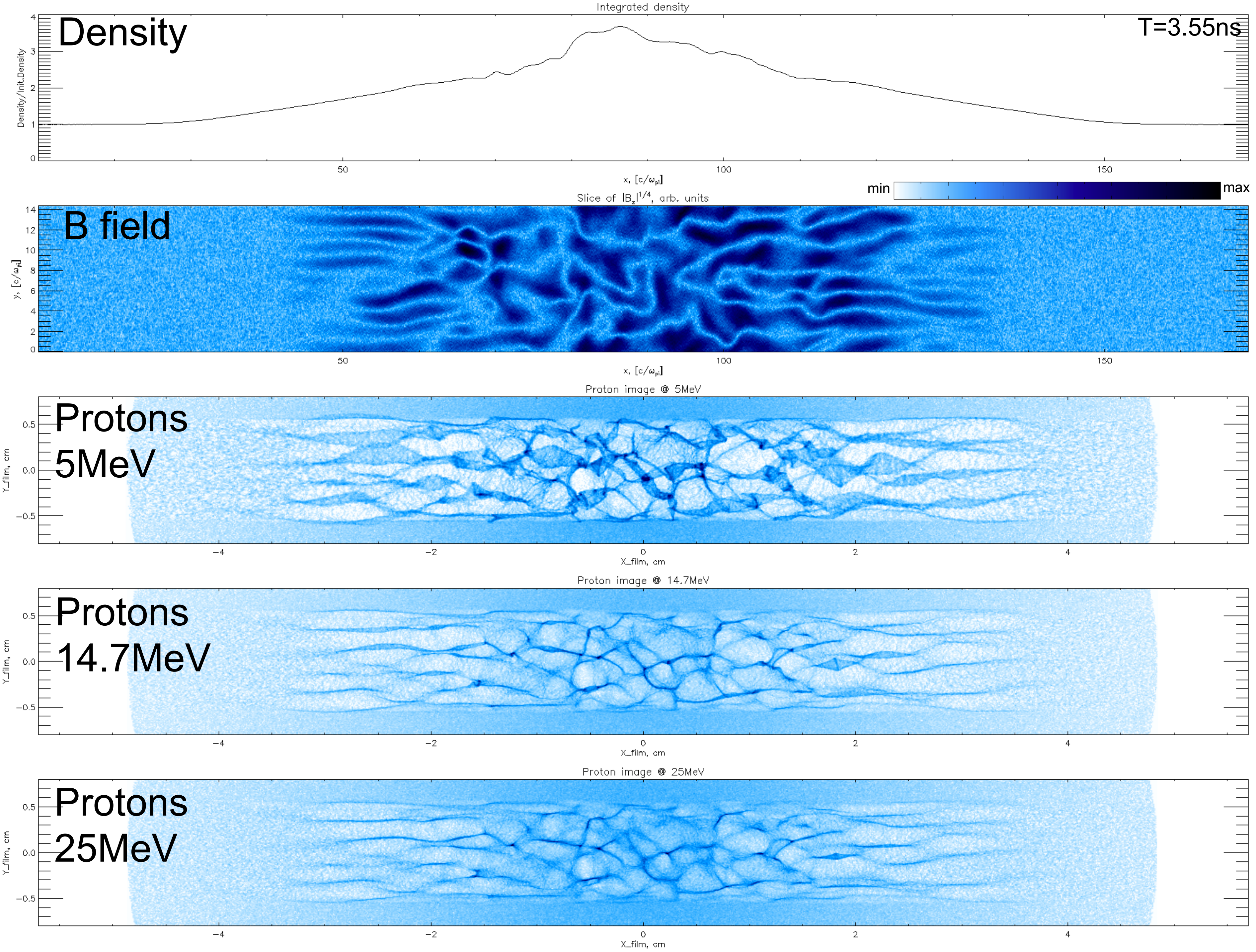
Integrated density
Density
T=3.55ns
Density/Init.Density
0
1
2
3
4
50
100
150
x, [c/ω_pi]
min
max
Slice of |B_z|^{1/4}, arb. units
B field
y, [c/ω_pi]
0
2
4
6
8
10
12
14
50
100
150
x, [c/ω_pi]
Proton image @ 5MeV
Protons
5MeV
Y_film, cm
0.5
0.0
−0.5
−4
−2
0
2
4
X_film, cm
Proton image @ 14.7MeV
Protons
14.7MeV
Y_film, cm
0.5
0.0
−0.5
−4
−2
0
2
4
X_film, cm
Proton image @ 25MeV
Protons
25MeV
Y_film, cm
0.5
0.0
−0.5
−4
−2
0
2
4
X_film, cm

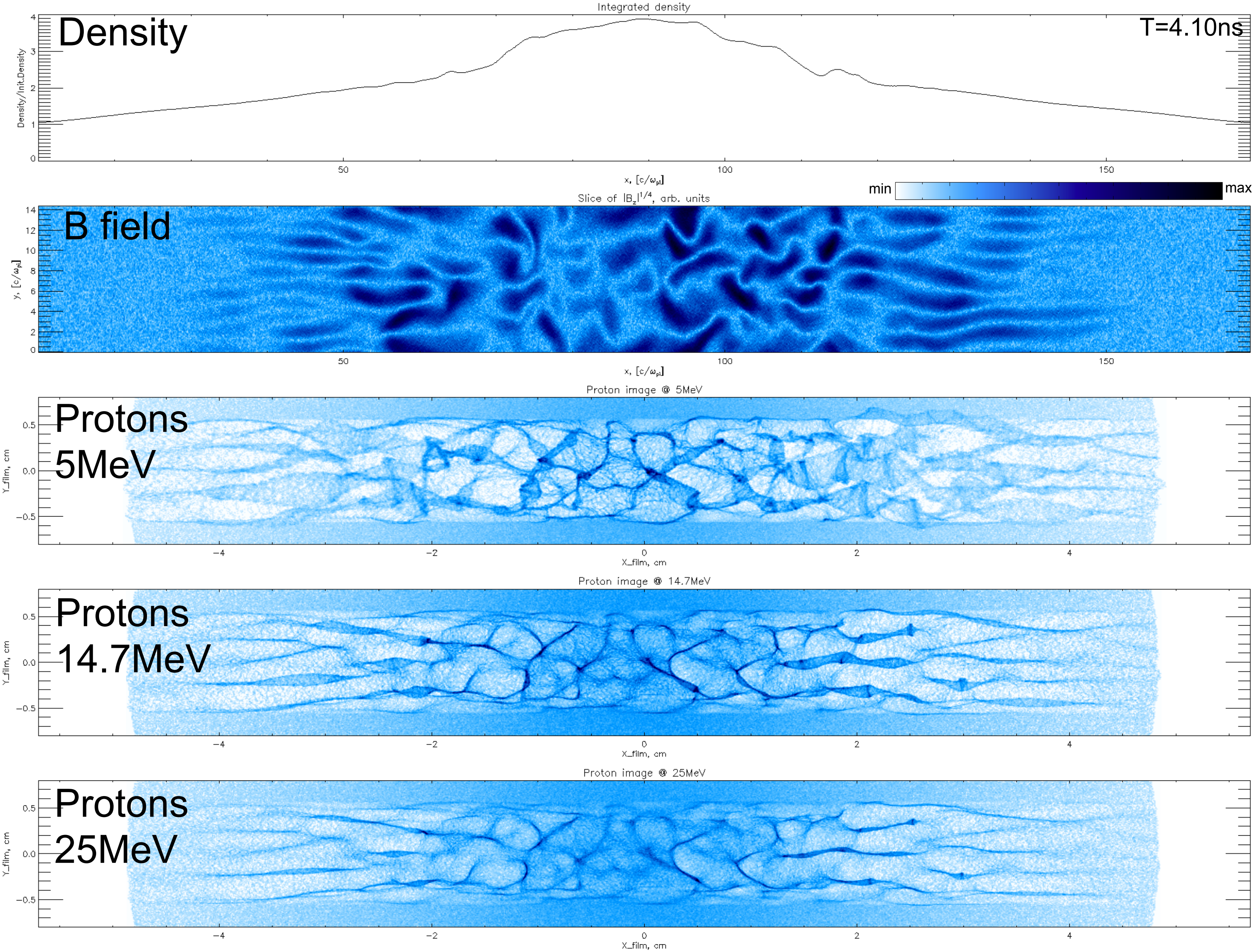
Integrated density
Density
T=4.10ns
Density/Init.Density
0
1
2
3
4
50
100
150
x, [c/ω_pi]
min
max
Slice of |B_z|^1/4, arb. units
B field
y, [c/ω_pi]
0
2
4
6
8
10
12
14
50
100
150
x, [c/ω_pi]
Proton image @ 5MeV
Protons 5MeV
Y_film, cm
0.5
0.0
−0.5
−4
−2
0
2
4
X_film, cm
Proton image @ 14.7MeV
Protons 14.7MeV
Y_film, cm
0.5
0.0
−0.5
−4
−2
0
2
4
X_film, cm
Proton image @ 25MeV
Protons 25MeV
Y_film, cm
0.5
0.0
−0.5
−4
−2
0
2
4
X_film, cm

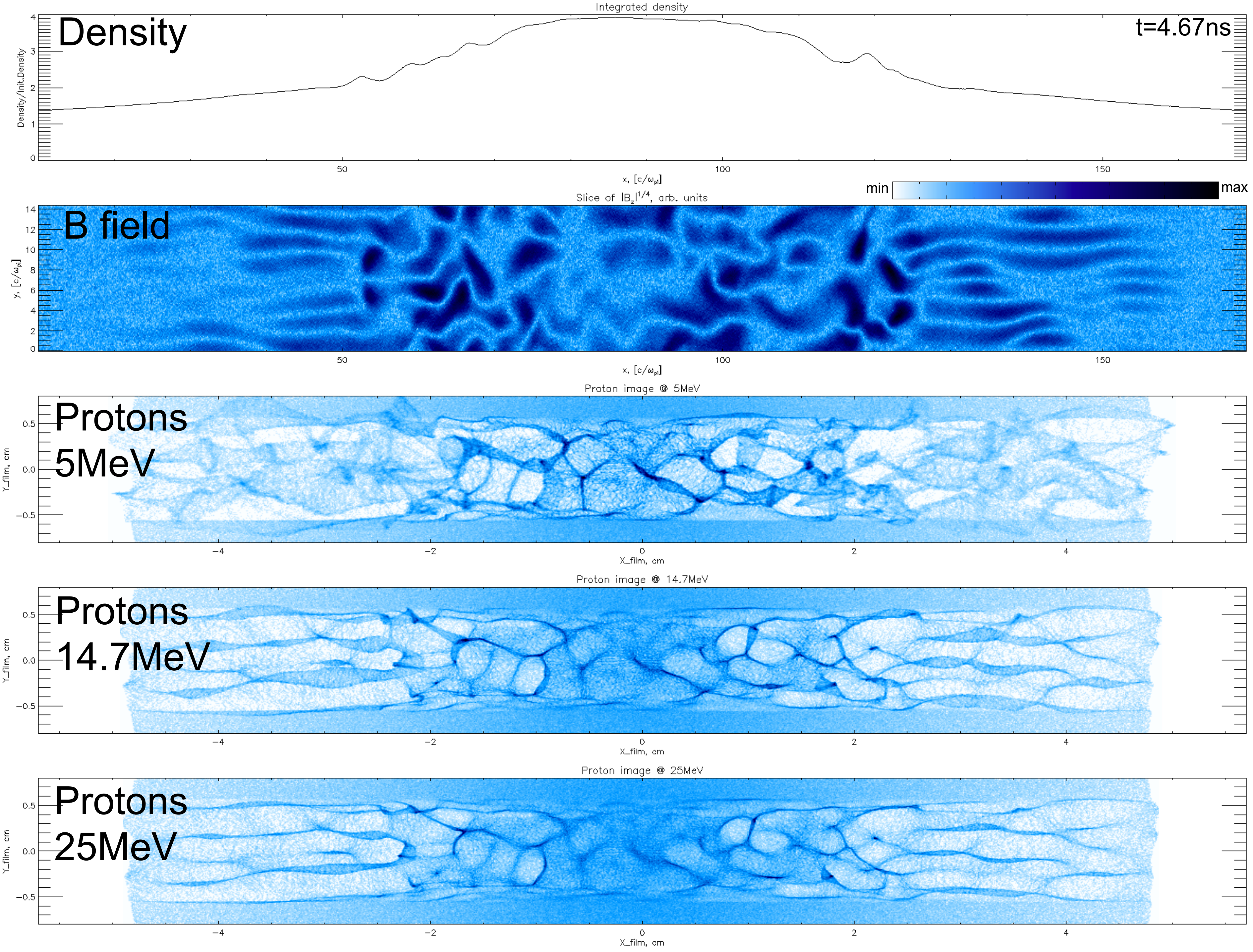
Integrated density
Density
t=4.67ns
Density/Init.Density
0
1
2
3
4
50
100
150
x, [c/ω_{pi}]
min
max
Slice of $|B_z|^{1/4}$, arb. units
B field
y, [c/ω_{pi}]
0
2
4
6
8
10
12
14
50
100
150
x, [c/ω_{pi}]
Proton image @ 5MeV
Protons
5MeV
Y_film, cm
0.5
0.0
−0.5
−4
−2
0
2
4
X_film, cm
Proton image @ 14.7MeV
Protons
14.7MeV
Y_film, cm
0.5
0.0
−0.5
−4
−2
0
2
4
X_film, cm
Proton image @ 25MeV
Protons
25MeV
Y_film, cm
0.5
0.0
−0.5
−4
−2
0
2
4
X_film, cm

Proton images at different times illustrate B-field evolution

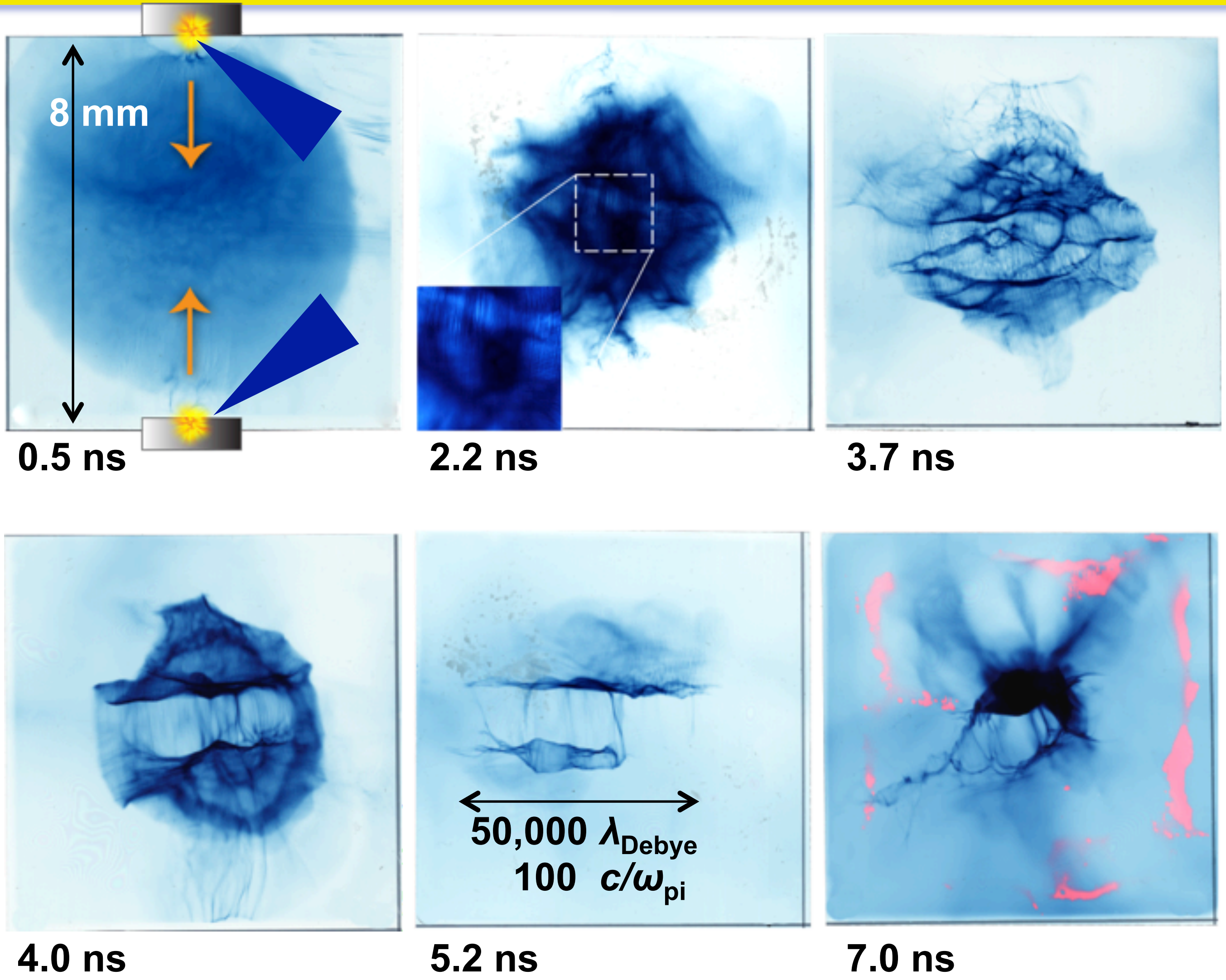

Proton images side-on view 7 to 8 MeV

Further work is needed to extend the spatial scales to allow for collisionless shock formation

Outline

- High-Energy-Density (HED) Plasma
  - US facilities

Zylstra et al.
(MIT)

- Plasma Nuclear Science using ICF-like implosions
  - p-p chain at relevant Gamow energies

Drake,
Kuranz et al.
(UM)

- Laser-produced Magnetohydrodynamics
  - similarity conditions
  - Rayleigh-Taylor growth in core-collapse SNe

Park,
Huntington et al.
(LLNL)

- Laser-produced Jets
  - ‘collisionless’ shocks
  - supersonic jet dynamics

Manuel,
Kuranz et al.
(UM)

Chen et al.
(LLNL)

- Pair-Plasma Production
  - relativistic jets
- Summary

Jets form during all stages of low-mass star formation

Collapsing pre-stellar dense core

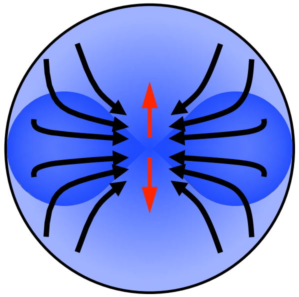

Time in Years 0 ~10^5 ~10^6

beginning of an outflow

Cloud Radius	**~ 10^4 AU**
Cloud Mass	**~ few $M_\odot$**
Accretion Rate	**~ 10^{-4} $M_\odot$/year**

Jet/Outflow:

- **Young pre-stellar (adiabatic?) core**
- **Estimated age 200 years**
- **Slow, few km/s outflow**

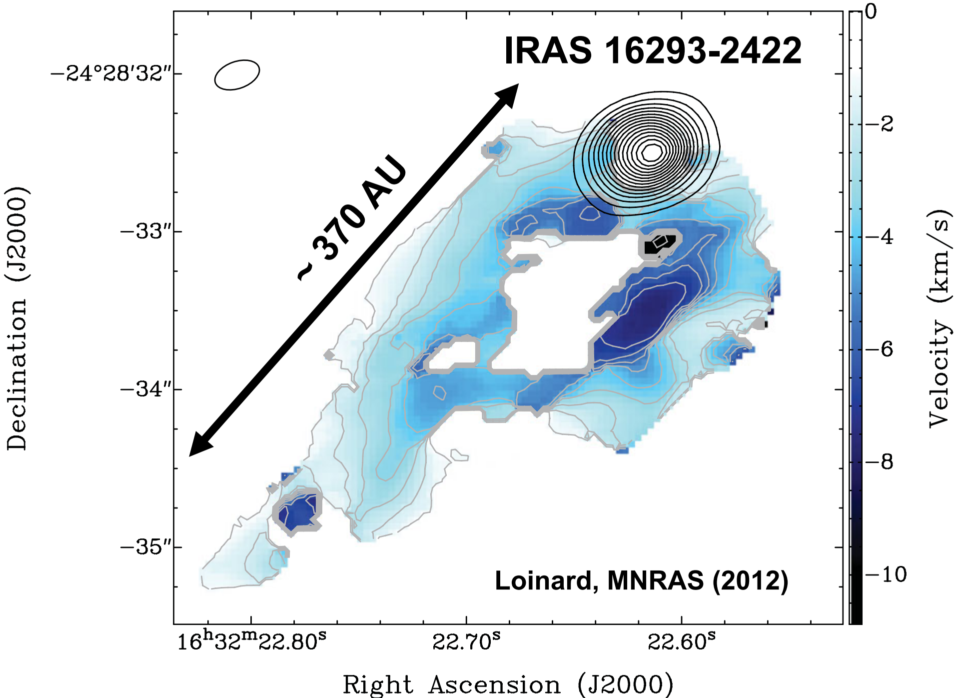

IRAS 16293-2422

Loinard, MNRAS (2012)

Jets form during all stages of low-mass star formation

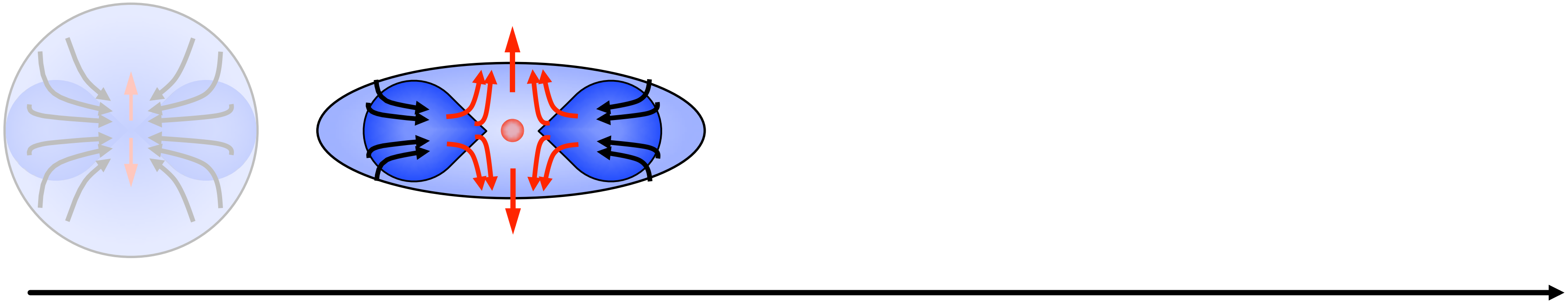

Collapsing pre-stellar dense core

Class 0
Young Accreting Protostar

Time in Years **0** **~10^5**

beginning of an outflow

jet/outflow ~ sub-pc scale

Envelope Radius ~ 10^3 AU
Envelope Mass > $M_\star$
Accretion Rate ~ 10^{-5} $M_\odot$/year

Jet/Outflow:

- **Typically observed as molecular flows from the source**
  - **Slow (< 10 km/s) cavities**
  - **Fast (~10-100 km/s) jets**

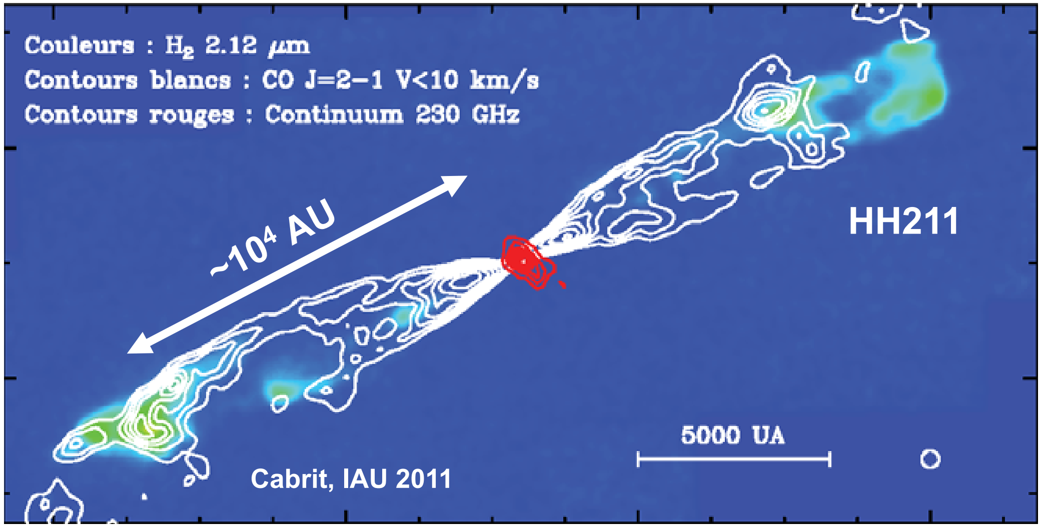

Cabrit, IAU 2011

Jets form during all stages of low-mass star formation

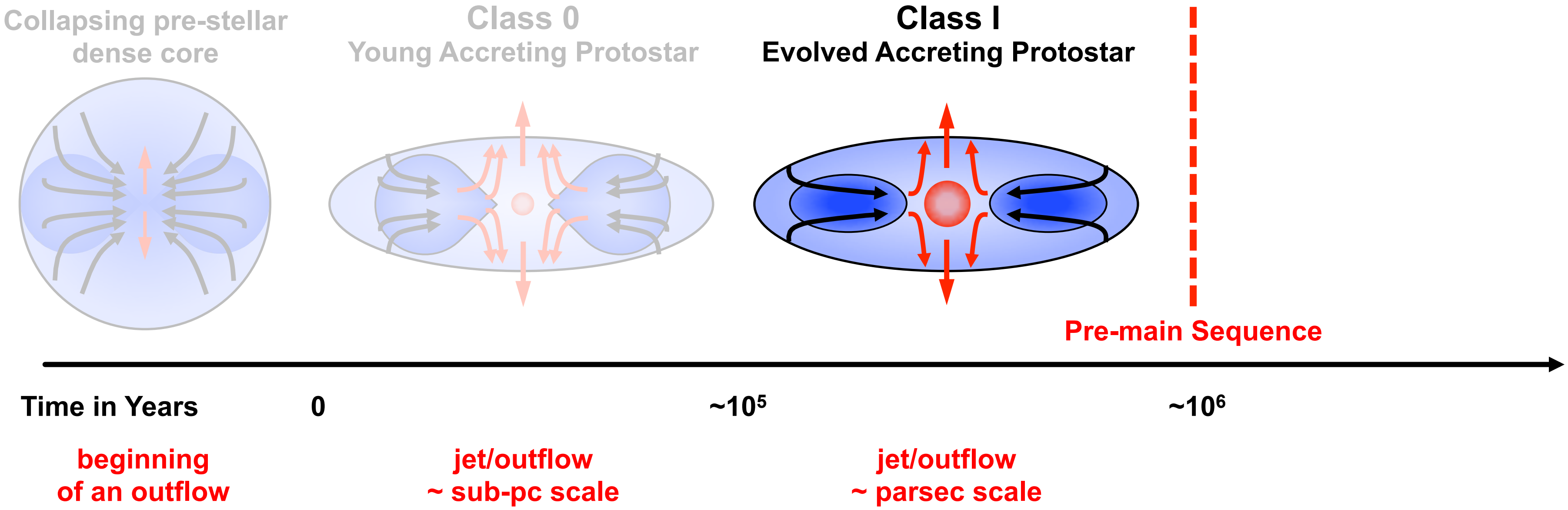

Collapsing pre-stellar dense core

Class 0
Young Accreting Protostar

Class I
Evolved Accreting Protostar

Pre-main Sequence

Time in Years **0** **~10^5** **~10^6**

beginning of an outflow

jet/outflow ~ sub-pc scale

jet/outflow ~ parsec scale

Envelope Radius	**~ few ×10^2 AU**
Disk Mass	**$< M_\star$**
Accretion Rate	**~ 10^{-6} $M_\odot$/year**

Jet/Outflow:

- **Atomic jet traced to pc-scales**
- **Weaker swept up molecular flow**
- **Clear evidence of jet episodicity and variability**

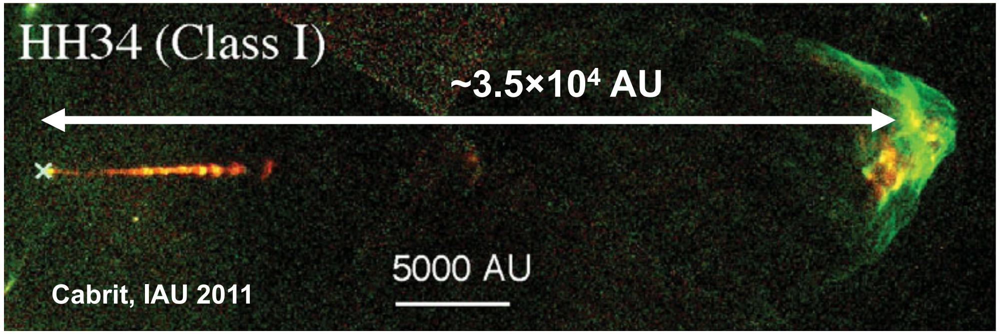

Cabrit, IAU 2011

Jets form during all stages of low-mass star formation

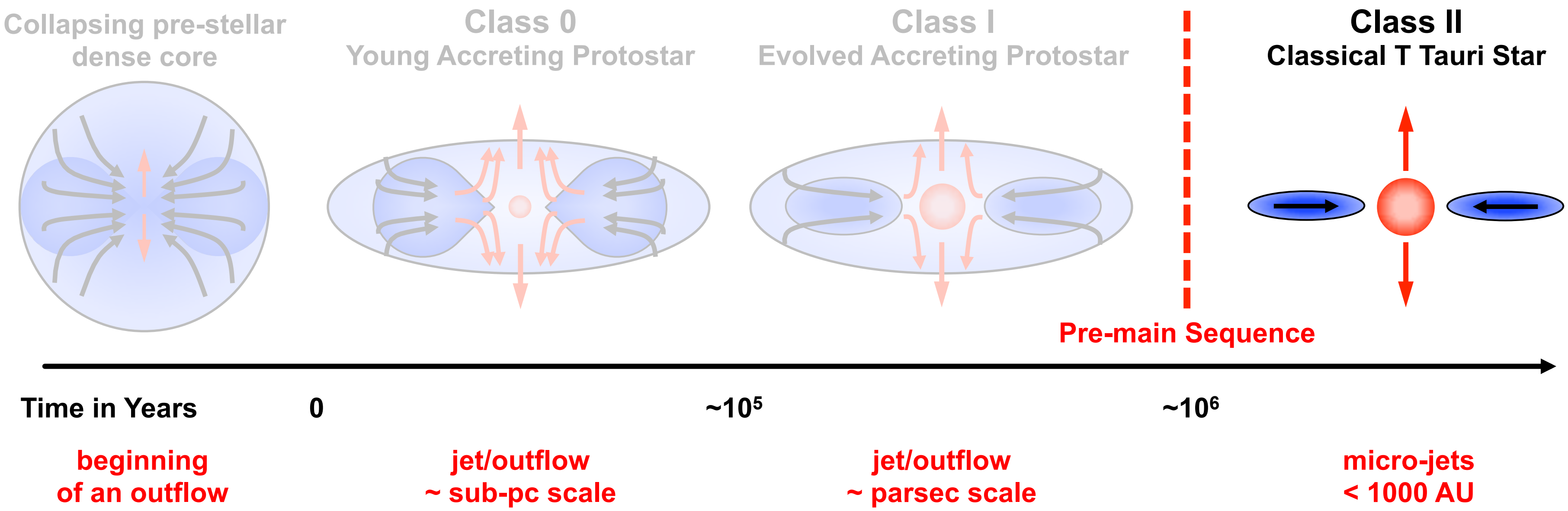

Collapsing pre-stellar dense core

Class 0
Young Accreting Protostar

Class I
Evolved Accreting Protostar

Class II
Classical T Tauri Star

Pre-main Sequence

Time in Years 0 ~10^5 ~10^6

beginning of an outflow

jet/outflow ~ sub-pc scale

jet/outflow ~ parsec scale

micro-jets < 1000 AU

Disk Radius	**~10^2 AU**
Disk Mass	**<< $M_\star$**
Accretion Rate	**~ 10^{-7} $M_\odot$/year**

Jet/Outflow:

- **Fast, few ×10^2 km/s atomic jets**
- **Wide-angle, slow H_2**
- **Rapid (few years) jet variability**

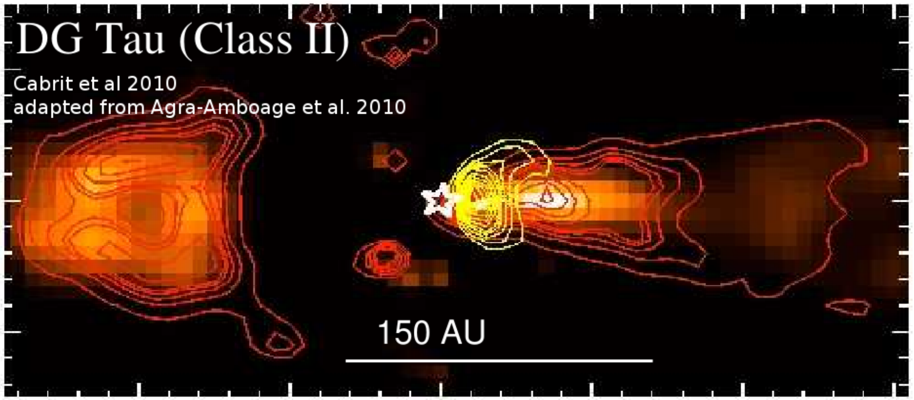

DG Tau (Class II)

Cabrit et al 2010
adapted from Agra-Amboage et al. 2010

Jets form during all stages of low-mass star formation

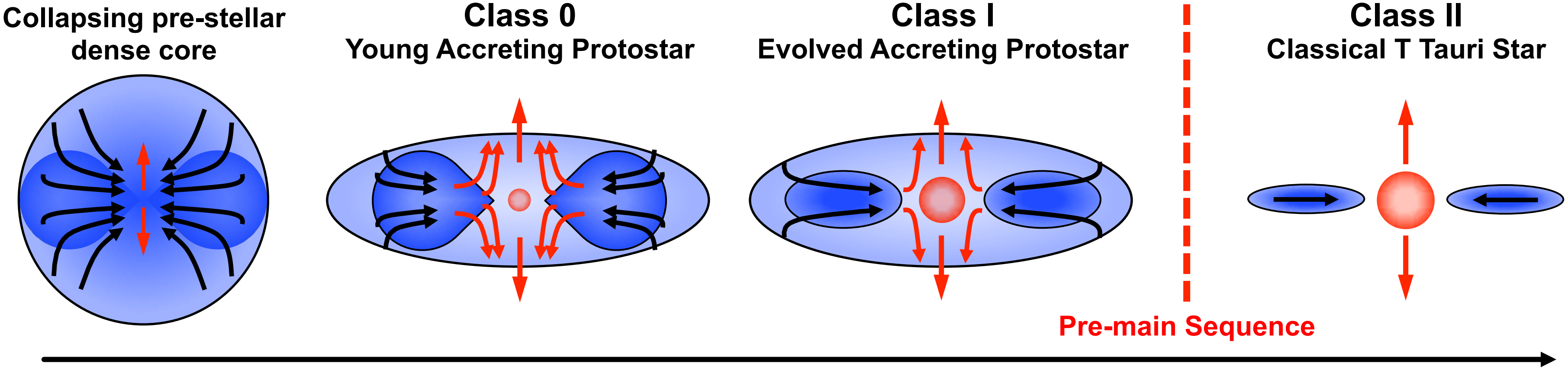

Collapsing pre-stellar dense core

Class 0
Young Accreting Protostar

Class I
Evolved Accreting Protostar

Class II
Classical T Tauri Star

Pre-main Sequence

Time in Years **0** **~10^5** **~10^6**

beginning of an outflow

jet/outflow ~ sub-pc scale

jet/outflow ~ parsec scale

micro-jets < 1000 AU

Jets form during all stages of evolution in accretion systems where $M_\star < 2\ M_\odot$

Cabrit, IAU (2011)

Magnetized plasma jets are prominent in young stellar objects with a wide range of parameters

Physical condition	Constraint	YSO Jets	Experiment
Viscosity plays minor role	Reynolds	$\sim 10^3$ - 10^7	$\sim 10^3$ - 10^5
Magnetic diffusion plays minor role	Magnetic Reynolds	$\sim 10^{13}$ - 10^{17}	$\sim 10^{-1}$ - 10^2
Supersonic flow	Mach number	$\sim 10^1$ - 10^2	$\sim 10^0$
Thermal compared to magnetic pressure	Thermal plasma β_{th}	$\sim 10^{-3}$ - 10^1	$\sim 10^0$ - 10^5
Dynamic compared to magnetic pressure	Dynamic plasma β_{dyn}	$\sim 10^{-3}$ - 10^1	$\sim 10^{-3}$ - 10^5

Curran et al., MNRAS 382 (2007); Carrasco-Gonzalez et al., Science 330 (2010); Ferreira AA 452 (2006); Reipurth ARAA 39 (2001)

Jets are produced from laser-irradiated plastic targets and magnetized using a custom-built solenoid

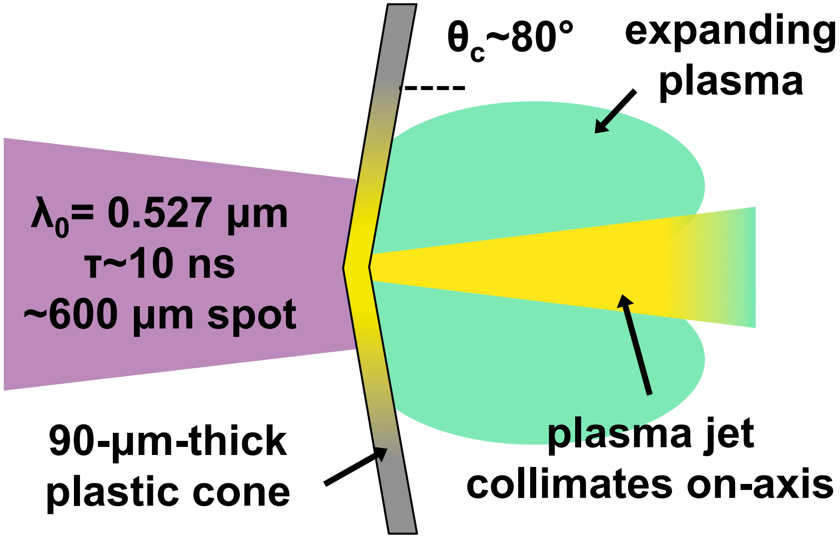

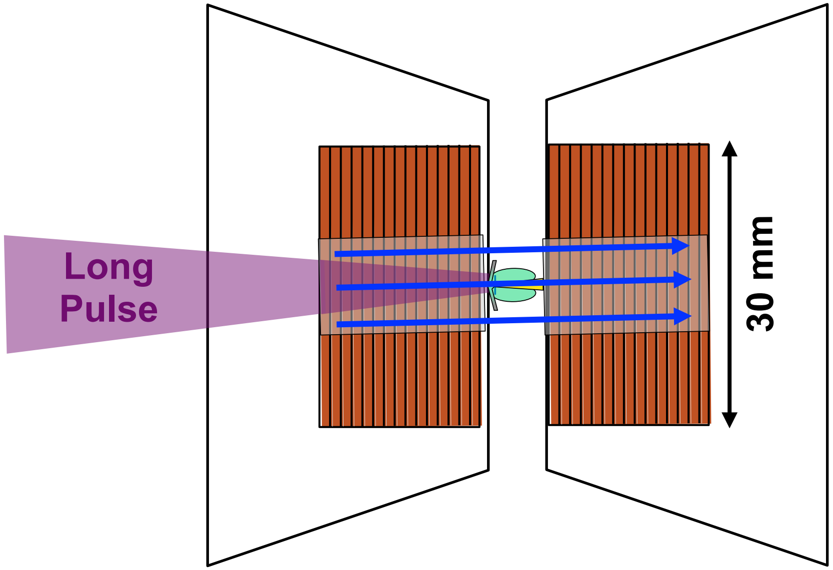

The 5 T point design generates thermal betas down to β~0.01-1 and dynamic betas down to to β~1-10
($n \sim 10^{18}$ cm^{-3}, T~1 eV, v~50-150 km/s)

Initial experiments focused on creating jets and investigated magnetization effects on jet morphology

Raw Interferogram
t~50 ns

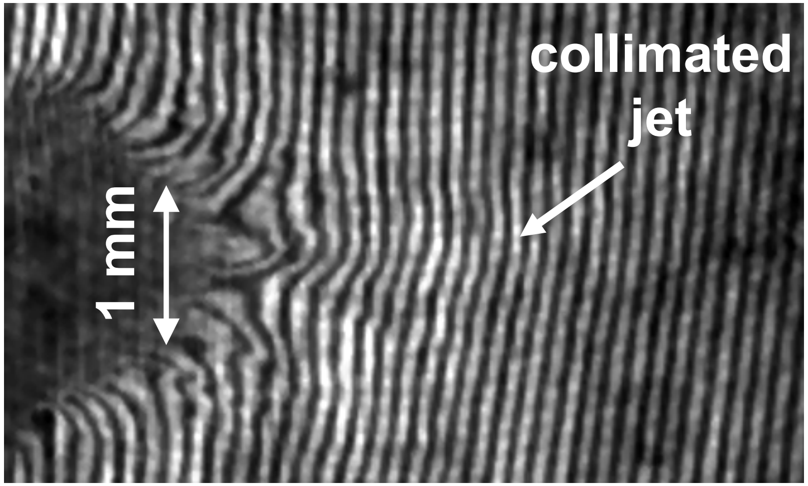

wavelet analysis

Unwrapped and Inverted
t~50 ns

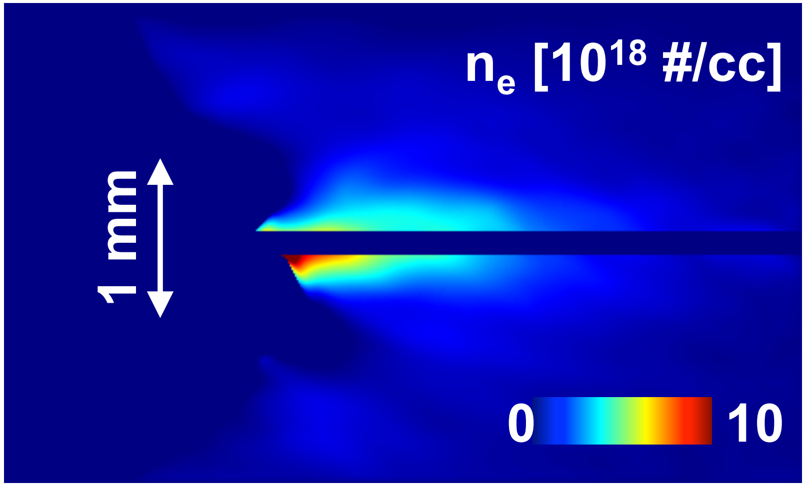

Interferometry indicates densities of n ~ 10^{18}-10^{19} cm^{-3} and demonstrates mm-scale hydrodynamic collimation

Collimated jets formed at varying drive energies

E ≈ 180 J

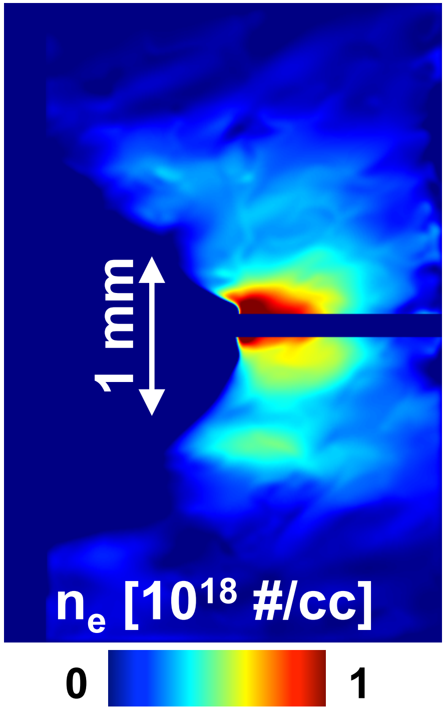

E ≈ 330 J

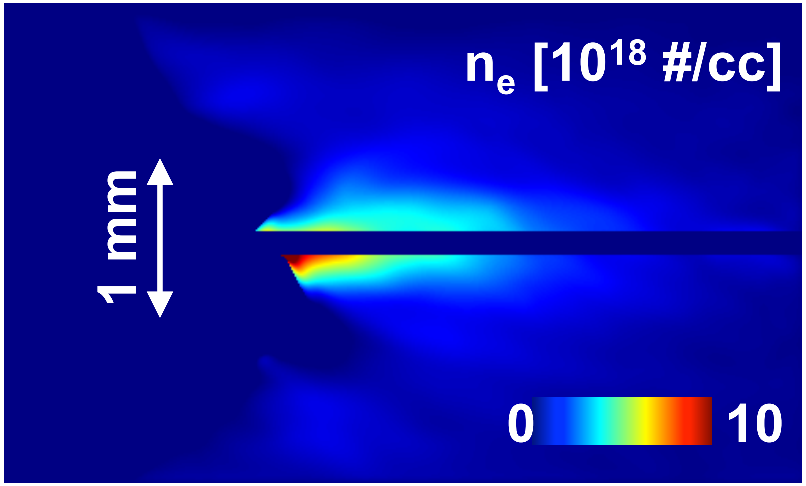

Free electron density is reduced at lower energies, but bulk jet characteristics are roughly constant:

- **collimated diameter is ~500 µm**
- **average axial velocity is ~40-50 µm/ns**

Complete disruption of the collimated jet was observed with an applied 5-T B-field along the jet axis

- **A hollow cavity is observed in electron density**
- **The cavity wall is ~300 µm thick and tapers from ~3 mm to ~2 mm in diameter**

---

* Manuel, HEDP (2014)

Cavity formation is very sensitive to the plasma-β

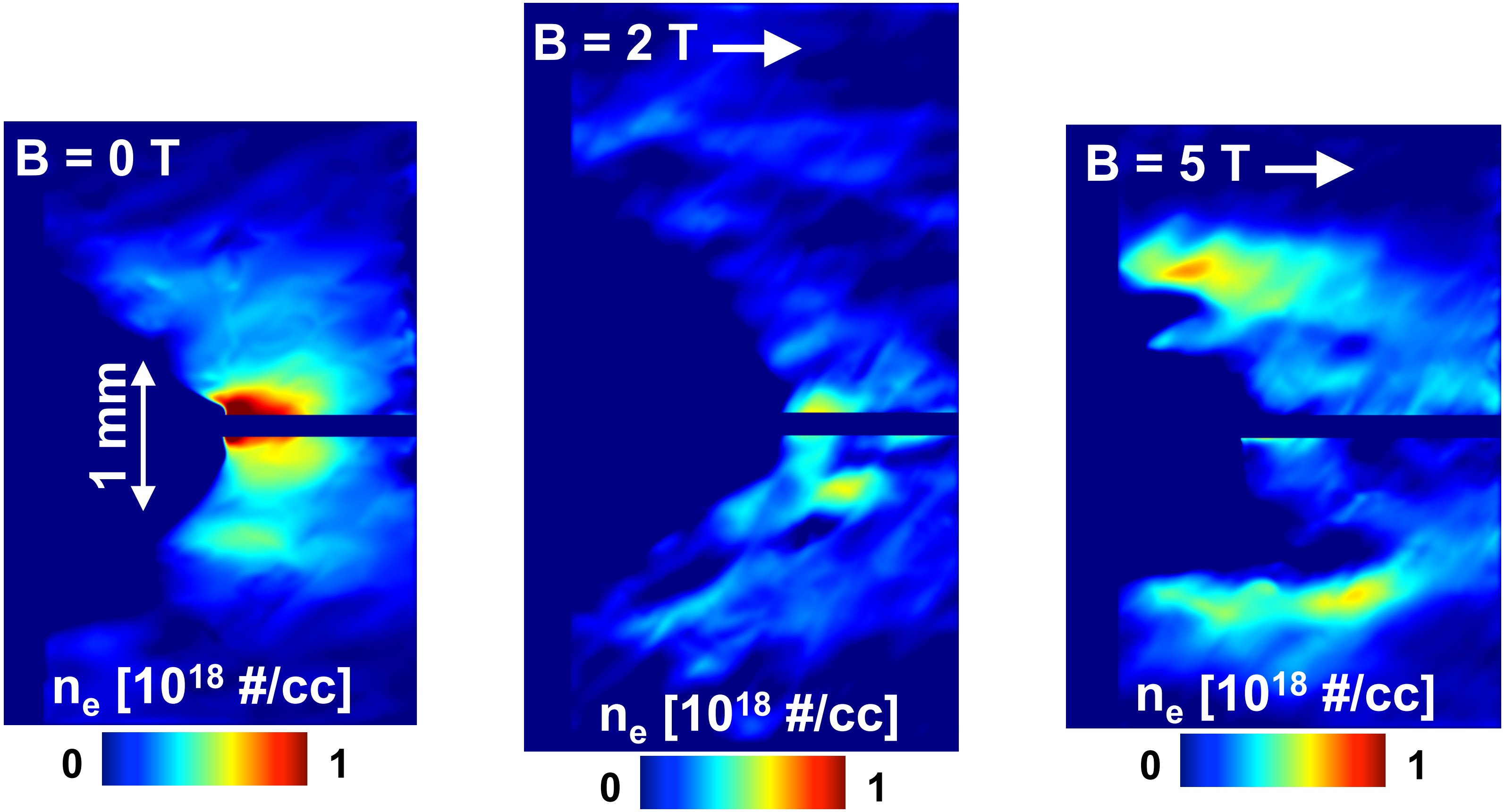

In the stellar analogs to these systems, collimated outflows from the star may be disrupted by the background field.

Previous work demonstrated cavity formation in an expanding plasma plume

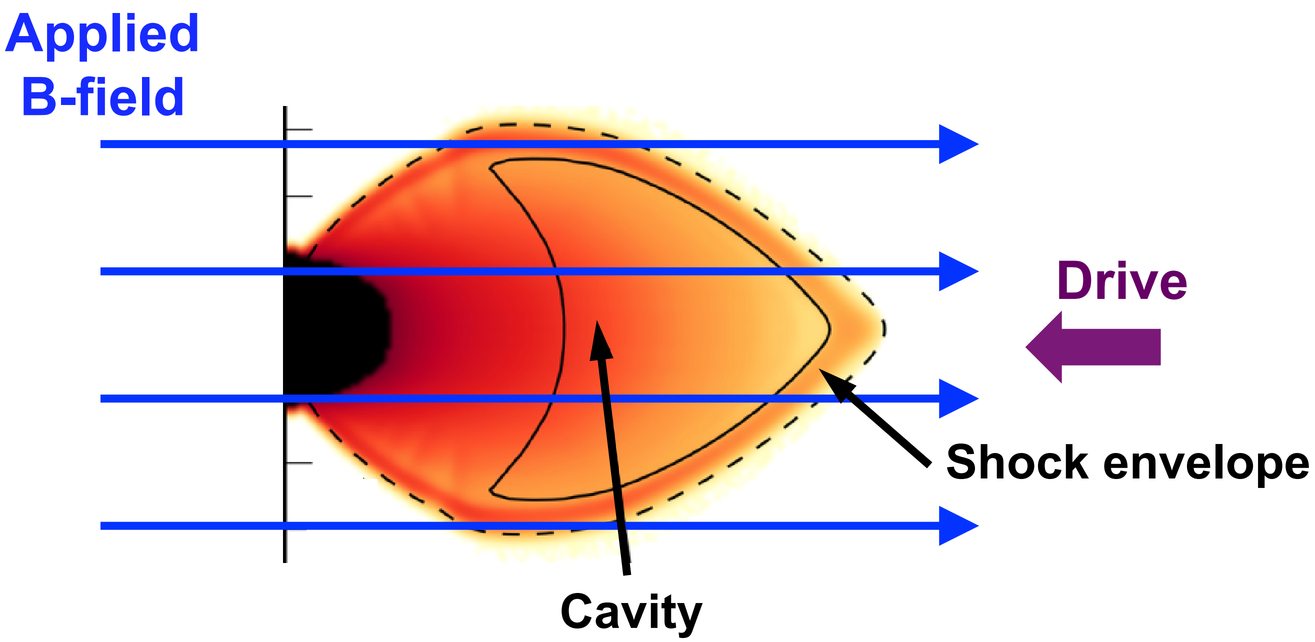

Radial expansion stops when $\rho v^2 \approx \frac{B^2}{2\mu_0}$

Ciardi *et al.* PRL 110 (2013) ; Albertazzi Science 346 (2014)

The initially expanding plasma is collimated by induction

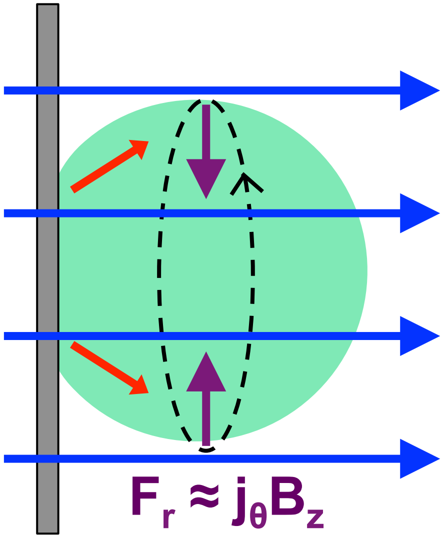

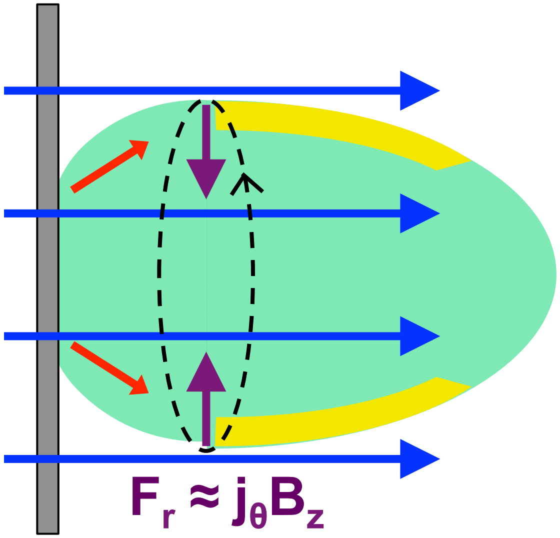

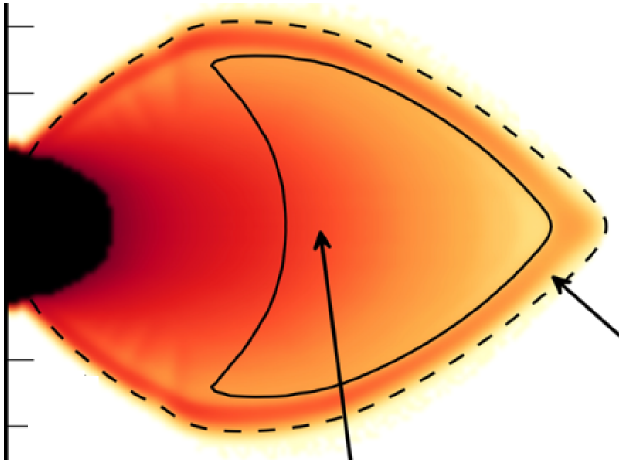

The initially expanding plasma is collimated by induction

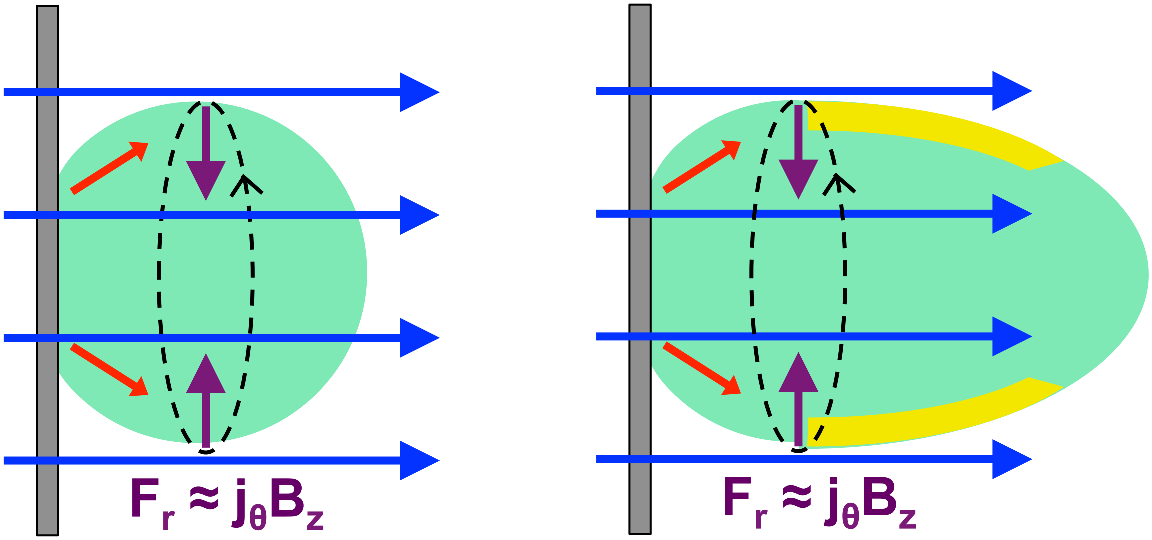

Induced toroidal current acts to oppose the change in flux

$$\eta j = -\frac{\partial}{\partial t}\int \mathbf{B}\cdot d\mathbf{A}$$

$$j_\theta(r) = -\frac{2\pi}{\eta}\int B_z v_r dr$$

The direction of the radial velocity in the plasma determines the induced current direction.

Central jet disruption and shock envelope formation may be simply caused by induction

Side View

Face-on View

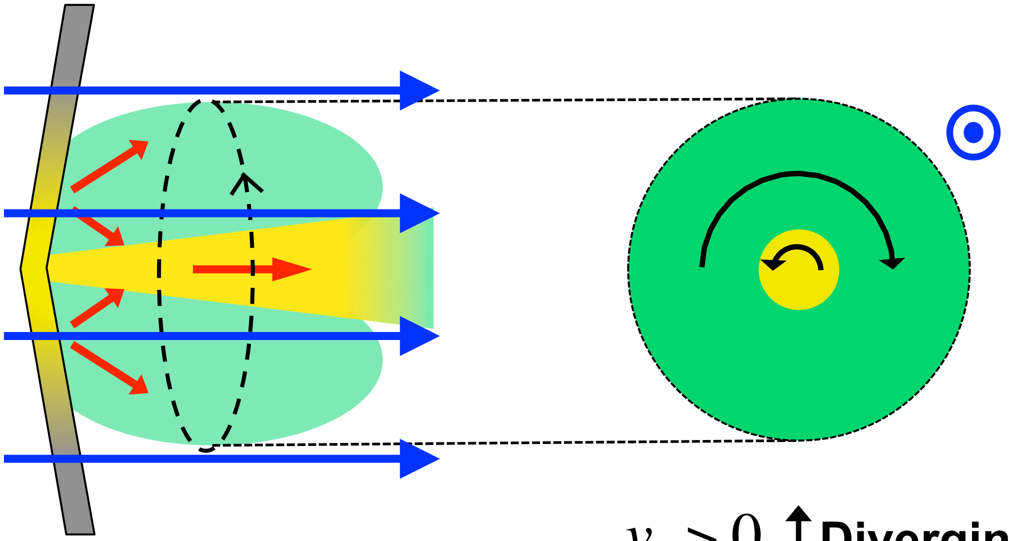

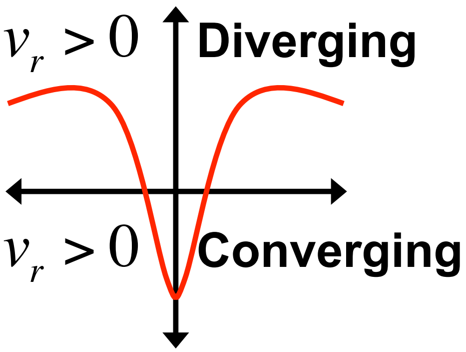

Induced toroidal current acts to oppose the change in flux

$$\eta j = -\frac{\partial}{\partial t}\int \mathbf{B}\cdot d\mathbf{A}$$

$$j_\theta(r) = -\frac{2\pi}{\eta}\int B_z v_r dr$$

$$F_r \approx -\frac{2\pi}{\eta} B_z^2 \int v_r dr$$

Central jet disruption and shock envelope formation may be simply caused by induction

Side View

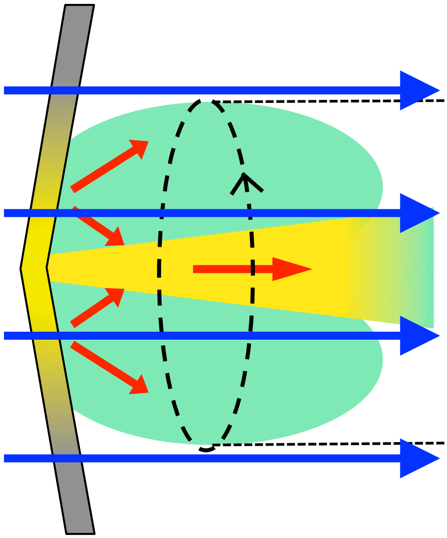

Face-on View

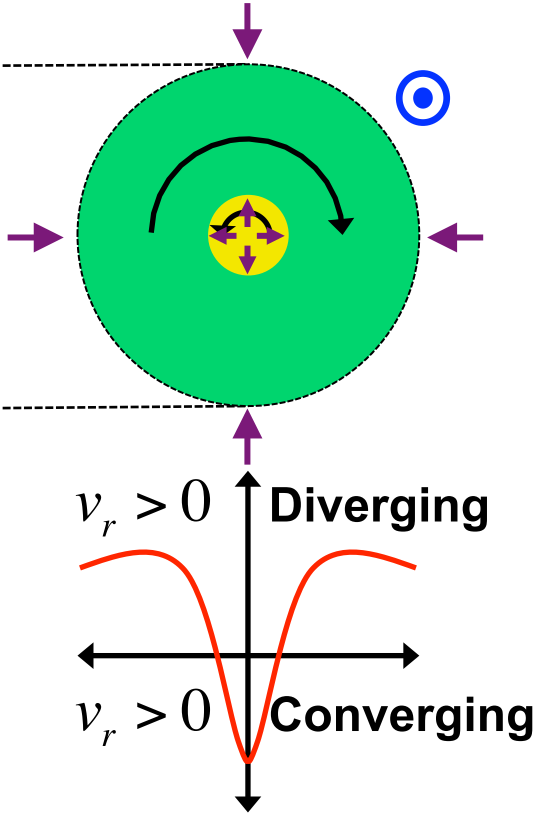

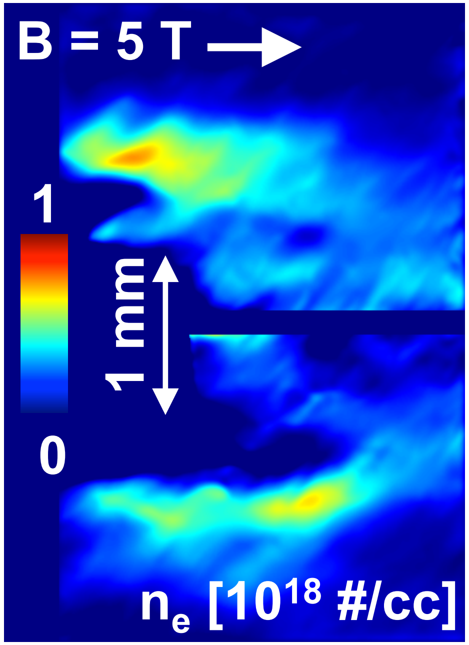

The J×B force does not permit axial collimation but still forms an envelope from the radially expanding plasma

Outline

- High-Energy-Density (HED) Plasma
  - US facilities

Zylstra et al.
(MIT)

- Plasma Nuclear Science using ICF-like implosions
  - p-p chain at relevant Gamow energies

Drake,
Kuranz et al.
(UM)

- Laser-produced Magnetohydrodynamics
  - similarity conditions
  - Rayleigh-Taylor growth in core-collapse SNe

Park,
Huntington et al.
(LLNL)

- Laser-produced Jets
  - ‘collisionless’ shocks
  - supersonic jet dynamics

Manuel,
Kuranz et al.
(UM)

Chen et al.
(LLNL)

- Pair-Plasma Production
  - relativistic jets

- Summary

Relativistic plasmas can be created using high-power-laser facilities

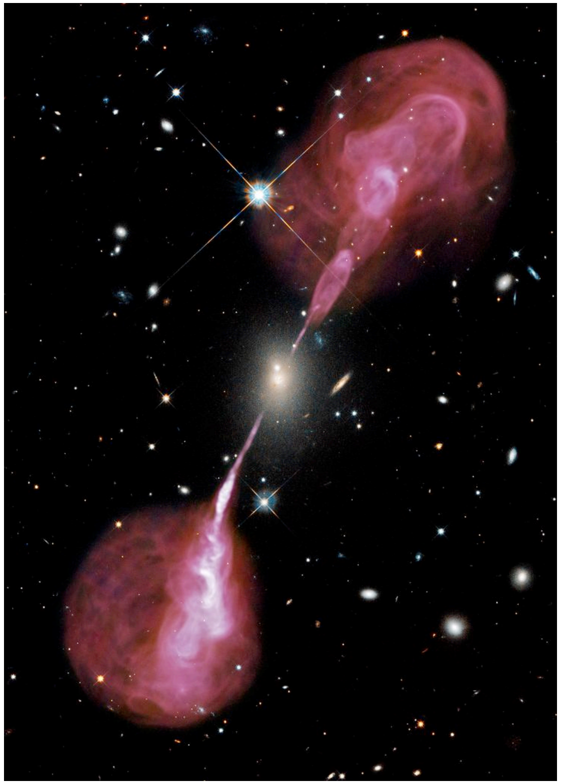

Unique features of these pair plasmas:

- **Positron acceleration**
- **Quasi monoenergetic positrons**
- **Relativistic electron-positron jets**
- **Scaling against laser energy**
- **Collimation**

Can we create and study relativistic jet dynamics in the lab?

At high laser intensities, photon-particle and particle-particle interactions become relativistic

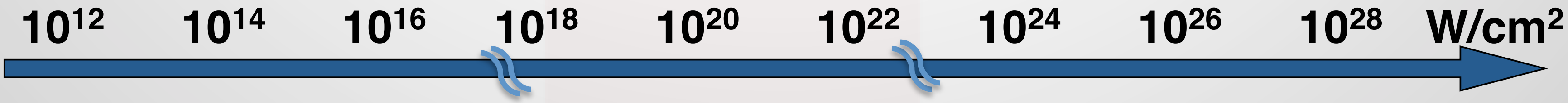

- atomic processes
- collisional absorption
- non-linear optics

- relativistic electrons
- nuclear processes
- γ-production
- e^+e^- plasmas

- pion production
- relativistic protons
- QED

Typical parameters	**> 10^{20} W/cm^2**
Electric fields	10^{12} V/m
Magnetic fields	100's MG
Pressure	Gbar
Temperature	keV or 10^7 K
Acceleration	10^{21} g
Density	Nc or solid

Lasers create positrons indirectly through two processes using targets with high atomic numbers

Bethe-Heitler Process

$$\sigma_{BH} \propto Z^4$$

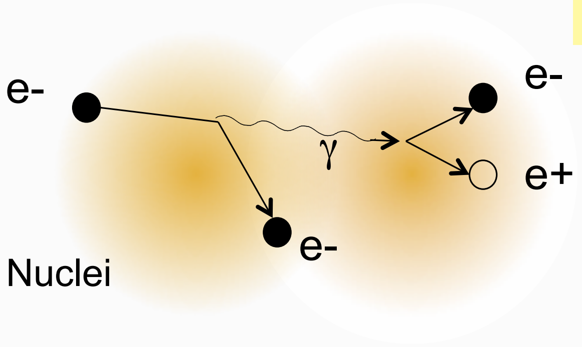

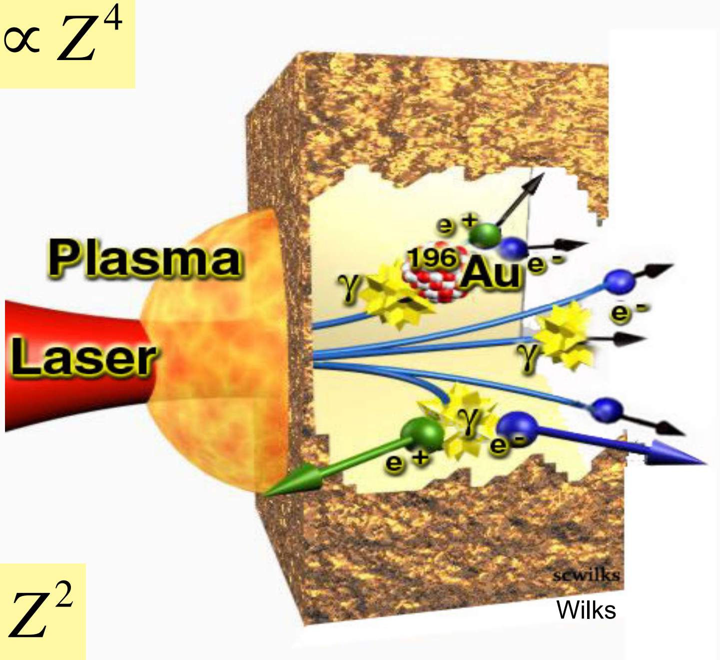

Wilks

Trident process

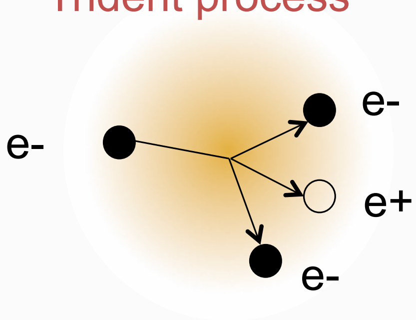

$$\sigma_{Tri} \propto Z^2$$

Heitler, 1954

Pair production probability is greatly enhanced by the nuclear field as momentum conservation is more easily preserved.

Laser-produced relativistic particles form jets at the back of the target

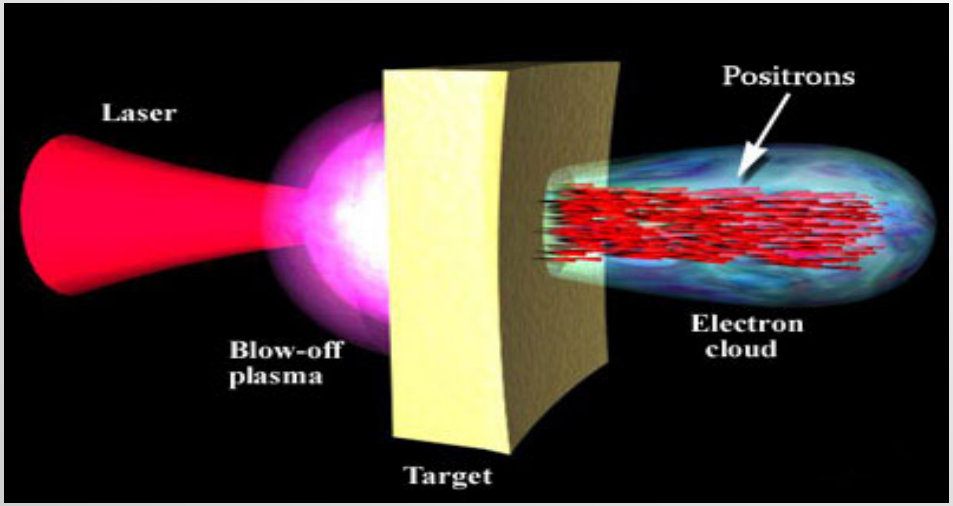

S. Wilks

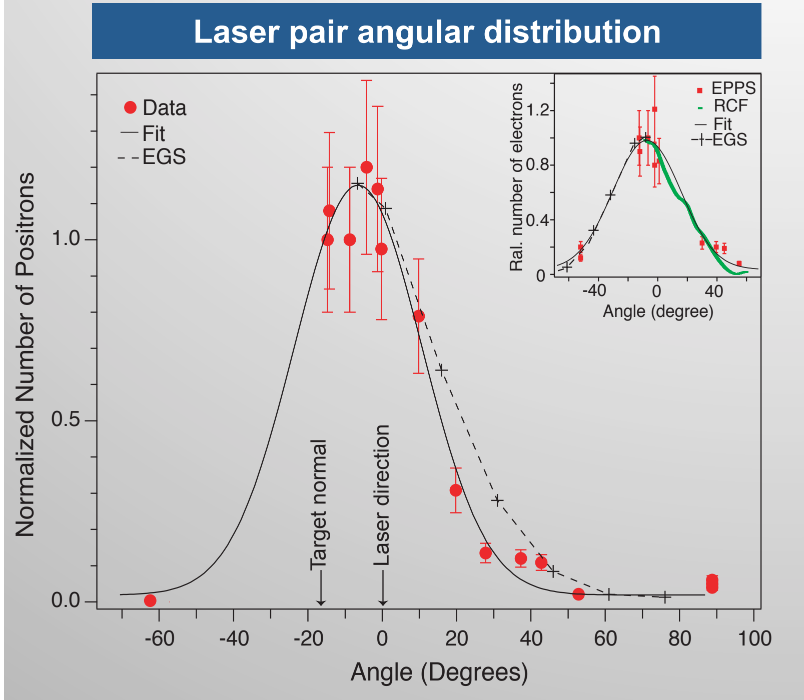

Chen *et al.*, PRL 2010

Jet angular spread is ~20°-30° and is shaped by electromagnetic fields in the target.

Relativistic particles can be further collimated by applying an external magnetic field

Simulation of positrons in MIFEDS B-fields

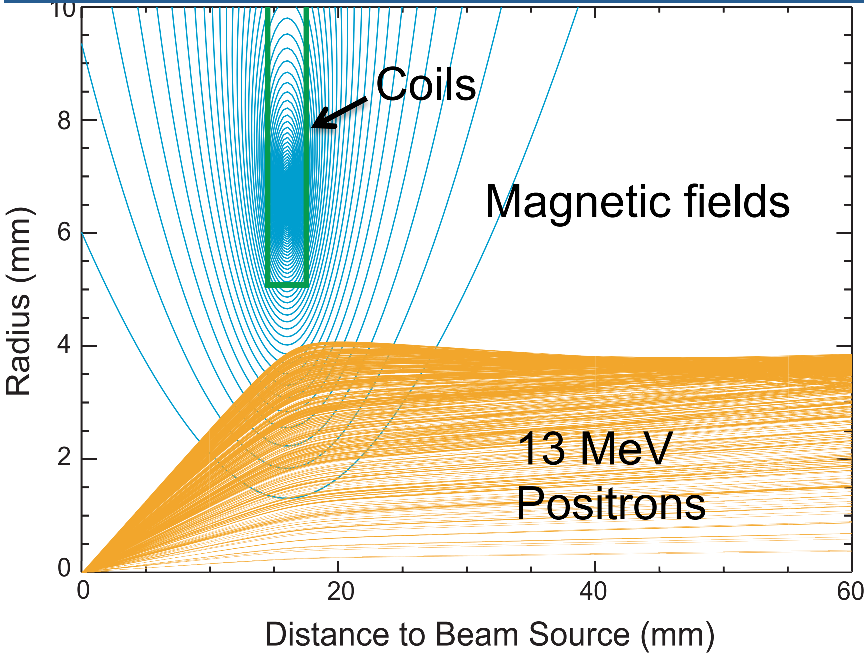

Simulation by G. Fiksel

Positrons & electrons spectra w/o collimation

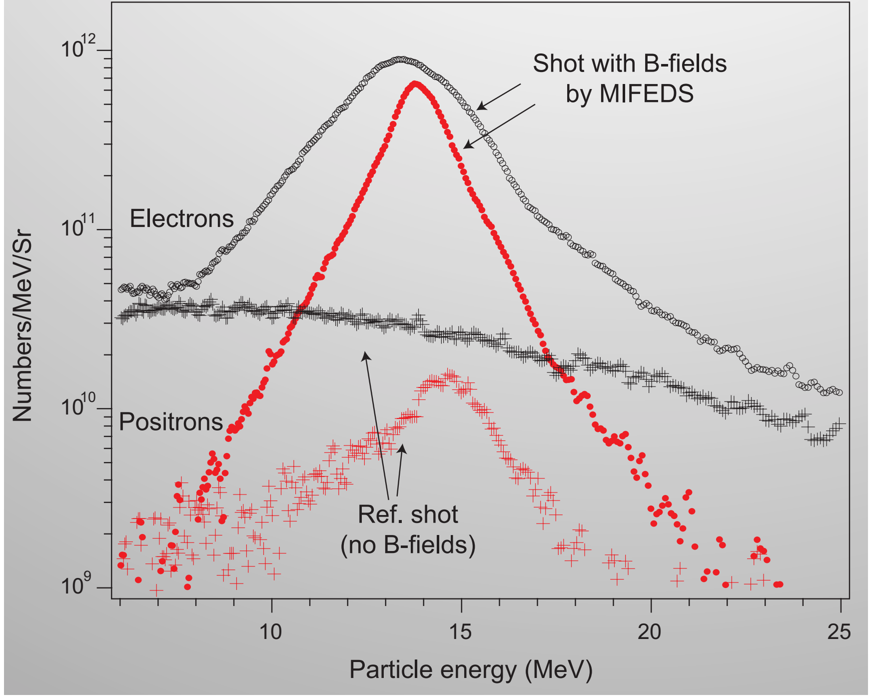

The effective divergence is reduced to 5° and the charge ratio (e-/e+) has reduced from ~100 to ~5

Laboratory experiments provide a complimentary technique to investigate some astrophysical systems

- High-power laser facilities provide a unique opportunity to generate physical conditions similar to those in various astrophysical systems

- Laboratory results are directly scalable when similarity and geometric conditions hold between the two systems

- Experiments also allow for detailed benchmark comparisons with numerical calculations in relevant dynamic regimes

Questions?